University of Plymouth

PEARL **https://pearl.plymouth.ac.uk**

Faculty of Science and Engineering | School of Geography, Earth and Environmental Sciences

2018-05

Fluvial system dynamics derived from distributed sediment budgets: perspectives from an uncertainty-bounded application

Downs, PW

http://hdl.handle.net/10026.1/10757

10.1002/esp.4319
Earth Surface Processes and Landforms
Wiley

All content in PEARL is protected by copyright law. Author manuscripts are made available in accordance with publisher policies. Please cite only the published version using the details provided on the item record or document. In the absence of an open licence (e.g. Creative Commons), permissions for further reuse of content should be sought from the publisher or author.

"This is the author's accepted manuscript. The final published version of this work (the version of record) is published by J.Wiley & Sons in *Earth Surface Processes and Landforms* available at: DOI: 10.1002/esp.4319. This work is made available in accordance with the publisher's policies. Please refer to any applicable terms of use of the publisher."

Fluvial system dynamics derived from distributed sediment budgets: perspectives from an uncertainty-bounded application

Peter W. Downs[1, 2], Scott R. Dusterhoff[3], Glen T. Leverich[4], Philip, J. Soar[5], Michael B. Napolitano[6]

[1]School of Geography, Earth and Environmental Sciences,

Plymouth University, Plymouth, PL4 8AA, UK

Tel: 01752 584990; Fax: 01752 585998;

peter.downs@plymouth.ac.uk

[2]Stillwater Sciences, 2855 Telegraph Ave #400, Berkeley, CA 94705, USA

[3]San Francisco Estuary Institute, 4911 Central Ave, Richmond, CA 94804, USA, USA

[2]Stillwater Sciences, 108 NW Ninth Avenue #200, Portland, OR 97209, USA

[5]Department of Geography, University of Portsmouth, Portsmouth, PO1 3HE, UK

[6]San Francisco Bay Regional Water Quality Control Board, 1515 Clay Street, Suite 1400, Oakland, CA 94612, USA

Keywords: fluvial geomorphology, sediment budget, uncertainty assessment, California, Anthropocene

Abstract

The utility of sediment budget analysis is explored in revealing spatio-temporal changes in the sediment dynamics and morphological responses of a fluvial system subject to significant human impacts during the recent Anthropocene. Sediment budgets require a data-intensive approach to represent spatially-differentiated impacts adequately and are subject to numerous estimation uncertainties. Here, field and topographic surveys, historical data, numerical modelling and a representative-area extrapolation method are integrated to construct a distributed, process-based sediment budget that addresses historical legacy factors for the highly regulated Lagunitas Creek (213 km^2), California, USA, for the period 1983–2008. Independent corroboration methods and error propagation analysis produce an uncertainty assessment unique to a catchment of this size. Current sediment yields of ~20,000 t a^{-1} ± 6,000 t a^{-1} equate to unit rates of ~300 t km^{-2} a^{-1} ± 90 t km^{-2} a^{-1} over the effective sediment contributing area of 64 km^2. This is comparable to yields associated with early Euro-American settlement in the catchment, despite loss of sediment supply upstream of the two large dams. It occurs because ~57% of the sediment is now derived from incision-related channel erosion. Further, the highly efficient routing of channel-derived sediments in these incised channels suggests an efflux of 84% of contemporary sediment production, contrasting with the efflux of ≈10–30% reported for unregulated agricultural catchments. The results highlight that sediment budgets for regulated rivers must accommodate channel morphological responses to avoid significantly misrepresenting catchment yields, and that volumetric precision in sediment budgets may best be improved by repeat, spatially dense, channel cross-section surveys. Human activities have impacted every aspect of the sediment dynamics of Lagunitas Creek (production, storage, transfer, rates of

movement through storage), confirming that, while distributed sediment budgets are data demanding and subject to numerous error sources, the approach can provide valuable insights into Anthropocene fluvial geomorphology.

1. INTRODUCTION

The sediment dynamics of modern-day fluvial systems reflect a combination of both autogenic changes, inherent to the natural geomorphologic functioning of the system, and a suite of allogenic changes related to such forcing factors as climate change and human influences (Hooke, 2000; Wilkinson, 2005; Macklin and Lewin, 2008, Downs *et al.*, 2013). While land use change may have been the pre-eminent influence on fluvial system changes for over a millennium in locations such as lowland Europe (*e.g.*, de Moor and Verstraeten, 2008; Brown, 2009), rapid population growth and industrialization over the last two hundred years mean that impacts are now often dominated by the consequences of actions related to water resources management, such as channelization, flow regulation and flood defence measures (Downs and Gregory, 2004; Gregory, 2006; Lewin, 2013). Assessing the extent and magnitude of human impact on contemporary sediment dynamics and morphological response of fluvial systems thus provides a measure of whether geomorphological systems have been subject to an overwhelming intensification of pressures (Brown *et al.*, 2013, 2017) argued to be an expression of the recent 'Anthropocene' (Meybeck, 2003; Crutzen and Steffan, 2003; Zalasiewicz *et al.*, 2010; Ruddiman, *et al.*, 2015). Such approaches require catchment-scale, high-resolution data to provide adequate spatial differentiation of sediment erosion sources, transport pathways and depositional volumes, and the use of numerous (often dissimilar) data sources to summarize the various historical legacy factors upon

77 which the study period is contingent (James *et al.*, 2009).

78

79 Sediment budgets can provide a powerful and sophisticated representation of
80 drainage basin sediment systems (Wasson, 2002; Warburton, 2011; Hinderer,
81 2012). Process-based sediment budgets, in particular, can enable the accurate
82 determination of spatially differentiated sediment production and yield, storages and
83 linkages as a function of catchment geologic, topographic and land use
84 characteristics (Reid and Dunne, 1996). Sediment budgets connect multiple
85 catchment sediment inputs (I) and changes in sediment storage (ΔS) with several
86 intermediate outputs (O) to result in a mass balance ($O = I \pm \Delta S$) that accounts for
87 spatial patterns of sediment production, storage, transfer and rates of movement
88 through storage for each relevant process within a catchment (Dietrich *et al.*, 1982).
89 The potential for sediment budgets to provide insights into the impact of changing
90 catchment conditions on fluvial system dynamics is widely appreciated (examples in
91 Reid and Dunne, 2016: Table 16.1) and has been the basis for several seminal
92 studies describing the impacts of historical human disturbance on sediment
93 processes (*e.g.*, Trimble, 1983, 2009). However, *distributed*, *process-based*
94 sediment budgets are data intensive and rarely constructed for catchments beyond
95 several square kilometres in drainage area, and even more rarely subject to an
96 estimation of their uncertainties. This is despite their argued applicability in resource
97 assessment (Reid and Dunne, 1996, 2016) and a tentative suggestion that sediment
98 budgets might provide a unifying framework for studies in geomorphology
99 (Slaymaker, 2003, 2008).

100

101 In the context of this apparently unfulfilled potential for using sediment budget

102 analyses in ‘beyond experimental scale’ catchments (*i.e*., those in which time- and
103 space-scales make it infeasible to monitor each process), the objectives here are
104 two-fold. First, to evaluate the interpretative utility of a distributed, process-based
105 sediment budget for revealing recent changes in fluvial system dynamics for a 10
106 km^2-scaled catchment and, second, to assess the value of uncertainty estimations in
107 similarly-focused decadal-scaled sediment budgets. A distributed, process-based
108 sediment budget is developed for Lagunitas Creek (California, USA), a 213 km^2
109 coastal catchment affected by land use change and flow regulation since Euro-
110 American settlement in the mid-Nineteenth century. The sediment budget
111 encompasses the period from Water Year (WY) 1983 to a final field survey in WY
112 2008. The starting date follows a 50-year storm event in WY 1982 that caused
113 widespread hillslope and channel erosion and also marks the completion of a project
114 to nearly double the storage capacity of a major water-supply reservoir in the
115 catchment, thus marking a step-change in the capacity for flow regulation and
116 sediment trapping. Combined, these events are suspected of creating a sustained
117 legacy in terms of catchment disturbance that will have dominated the recent period
118 and caused a complex suite of sediment process responses that are amenable to
119 examination as a spatially-distributed mass balance. Discussion centres on the
120 extent to which insights into the sediment dynamics of Lagunitas Creek are
121 achieved, and issues associated with uncertainty estimation for sediment budgets.
122

123 ## 2. STUDY AREA

124 Lagunitas Creek, set in the Coast Range geomorphic province of California (CGS,
125 2002), originates on the northern slopes of Mt. Tamalpais (peak elevation of 784 m

above sea level) and flows through a combination of oak and redwood forest, scrubland, and grazing lands before entering a broad tidal marsh at the head of Tomales Bay. The catchment is located within the San Andreas Rift Zone (Jennings, 1994) (**Figure 1**) and lateral displacement of the tectonically active landscape has locally offset drainage patterns while episodic earthquakes have triggered numerous hillslope failures. The most recent significant event occurred in 1906 (epicentre just west of the catchment on the San Andreas Fault), triggered thousands of landslides throughout the region (Youd and Hoose, 1978; Keefer, 1984) and may have a lasting impact on regional sediment yields (Vanmaercke *et al*., 2014). The underlying geology is mostly matrix-supported Franciscan mélange (age *ca.*100–160 MY), an erosion-prone sheared and deformed mixture largely composed of greywacke, argillite, shale, chert and metamorphic rocks, which produces a thin, moderately well drained, clay-rich loamy soil when weathered (Wentworth, 1997; Blake *et al.*, 2000; NRCS, 2007). The catchment is mostly rural and includes State and National Park lands; urban development has been focused primarily in the San Geronimo Creek sub-catchment. The mild Mediterranean climate is dominated by dry summers and wet winters (monthly mean temperatures 9–20 °C), including periods of intense rainfall frequently related to the El Niño Southern Oscillation (ENSO) (Fischer *et al*., 1996). Average annual precipitation is approximately 1,500 mm at Kent Lake (CDWR gauge #E10 4502 00: 1950 to 1999) *ca.*400 m above mean sea level.

Because landscape changes resulting from geomorphic process alterations can take many decades to complete, an understanding of fluvial system evolution requires knowledge of the historical factors most likely to have been driving geomorphological responses as context for interpreting changes observed in the most recent period

(Sear *et al.*, 1995; James *et al.*, 2009; James, 2010; Notebart and Verstraeten, 2010). Here, a combination of scientific literature and local historical information (*e.g.*, Niemi and Hall, 1996; SFBRWQCB, 2002; TBWC, 2003) suggests that, since the influx of Euro-American settlers in the mid-Nineteenth century, Lagunitas Creek

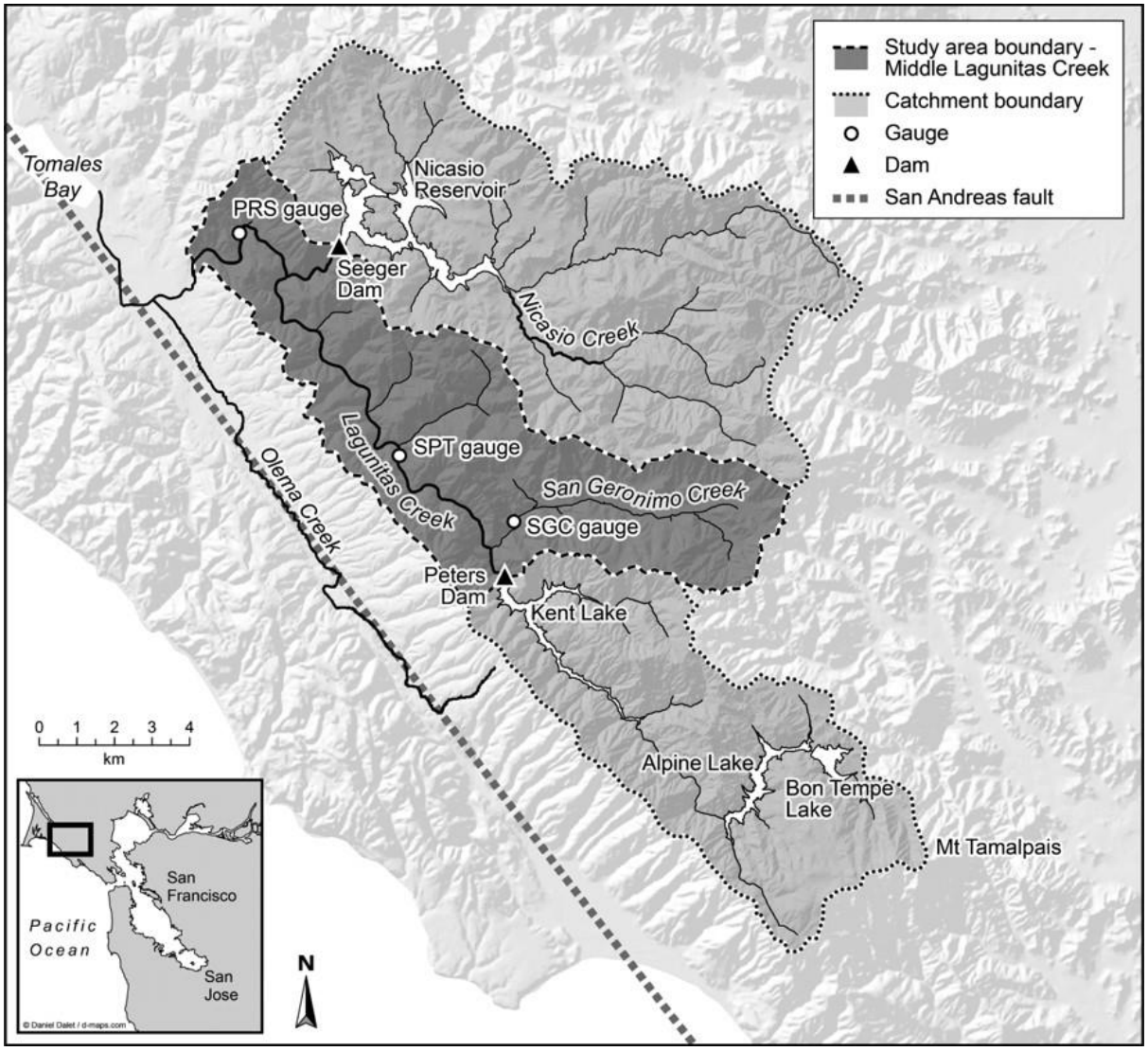

Figure 1: Drainage network of the Lagunitas Creek catchment and its vicinity. The Middle Lagunitas Creek area (highlighted) is now the effective sediment contributing area for the whole catchment: Peters Dam, impounding Kent Lake, and Seegar Dam impounding Nicasio Reservoir disconnect sediment delivery from the Upper Lagunitas Creek area and the Nicasio Creek catchment, respectively. Flow gauges: SGC = San Geronimo Creek; SPT = Samuel P. Taylor State Park; PRS = Point Reyes Station. Mt Tamalpais peaks at 784 m.

has been subject to four notionally distinct time periods of human influence (see **Figure 2**). In summary, the first period (1850–1918) began with the establishment of settlements within the San Geronimo Creek and Lagunitas Creek valleys and the development of crop production, ranching, and logging, and development of a small water-supply dam in 1872. The second period (1919–1945) included large-scale flow impoundments on Lagunitas Creek for water supply and a switch away from row crops to grazing. From 1945 to 1982, the third period involved a modest population increase throughout the catchment but a considerable increase in the extent of flow impoundment. This included the construction of the original Peters Dam (completed 1954) that regulates flow and sediment delivery from the Upper Lagunitas Creek catchment (55.7 km^2), and the completion of Seeger Dam (1961) that regulates flow and sediment delivery from almost all of the Nicasio Creek catchment (93.3 km^2). Finally, the period since 1983 included further impoundment achieved by raising Peters Dam (by nearly 14 m to 70 m total) and enactment of various regional and catchment policy initiatives intended to maintain or enhance environmental quality in relation to water quality, aquatic habitat and land development regulations.

Functionally, 70% of the 213 km^2 catchment now lies upstream of water-supply reservoirs and is disconnected for sediment supply. Thus, the effective contributing area of sediment production and downstream sediment connectivity in Lagunitas Creek catchment is now the 64.4 km^2 to the lowest streamflow gauging station, and is referred to herein as the Middle Lagunitas Creek. Middle Lagunitas Creek is unregulated in its upper 24 km^2 (the San Geronimo Creek sub-catchment), and is subject to increasing flow and sediment regulation moving downstream (see Figure 1).

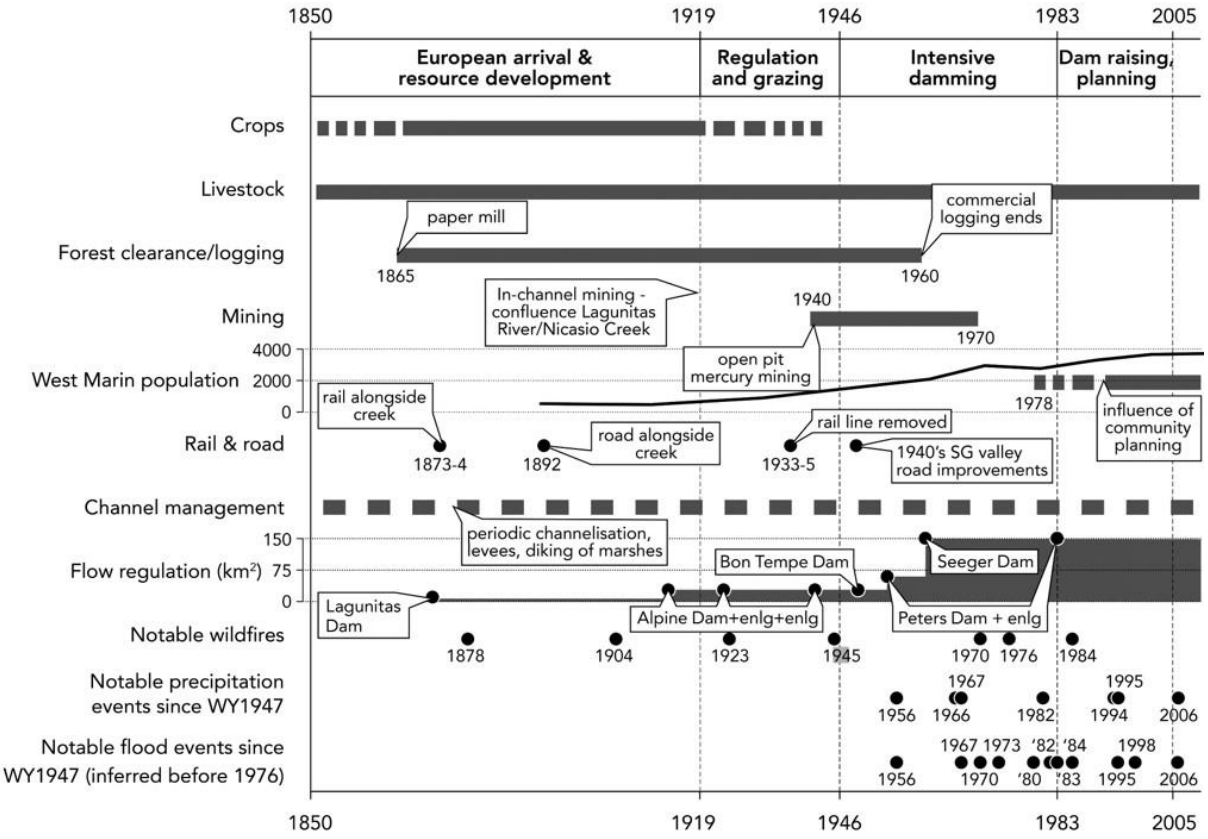

Figure 2 Chronology of major activity and disturbances in the Lagunitas Creek catchment with likely bearing on sediment budget processes (sources: Niemi and Hall, 1996; SFBRWQCB, 2002; TBWC, 2003). SG = San Geronimo, enlg = reservoir enlarged by raising the dam. Solid lines indicate known dates of activities, broken lines indicate intermittent activity or lack of date precision.

3. METHODS

For distributed sediment budgets, direct monitoring of all relevant sediment processes is increasingly difficult over catchment areas more than a few square kilometres due to inherent challenges in sampling feasibility and extrapolating results across larger areas (*e.g.*, Dietrich and Dunne, 1978). Alternatives include regional scale modelling (*e.g.*, Wilkinson et al., 2009) or, as here, methods that merge multiple field-based and historical data sources into comparable units of measurement, supplemented by terrain-based numerical modelling to estimate data from unmeasured processes. A suitable method of extrapolation is essential to

provide spatially distributed outputs. To begin, process-based sediment budgets require the identification of a finite suite of processes representative to the catchment's geomorphic province, thus ensuring that all the major processes are quantified (Dietrich *et al.*, 1982). Methods for estimating and validating processes judged most relevant to the California Coast Range geomorphic province are outlined below.

Discrete hillslope sources

Estimates of hillslope sediment production and delivery from discrete processes (*e.g.*, rill and gully erosion, shallow- and deep-seated landslides) were based on field surveys supplemented by aerial photograph analysis, with the production and delivery rates extrapolated to unsurveyed areas of the catchment within a GIS framework (details below). The occurrence, magnitude, and temporal development of discrete hillslope sediment production and delivery sources were examined using time-sequential aerial photographs (dated 1/82, 8/92, 3/00, 3/04: **Table 1**), in combination with two field surveys (2006 and 2008) and supplemental data from a 2002 survey of erosion sources in the San Geronimo sub-catchment (Stetson Engineers, 2002). Minimum recorded failure size was 1 m^2 during field surveys, and ~4 m^2 from aerial photographs, according to their resolution. Mass failures are generally initiated only during heavy rainfall: regional data collected after the notable storm event of 4th January 1982 identified a 24-hour event of *ca.*190–200 mm as sufficient to trigger debris-flow activity (Wilson and Jayco, 1997). Therefore, the study period likely encompasses three further hillslope erosion-generating events (Table 1), including one on 31st December 2005 (186 mm) that was observed during this study.

Table 1 - Aerial photography sets used in sediment production assessment

Photography date	Most recent 'significant' storm event	24-hr rainfall maximum (mm) [a]	Most recent river flood	Estimated peak flow ($m^3 s^{-1}$) [b]	Original scale	Photograph source [c]
7 Jan 1982	4 Jan 1982	268	4 Jan 1982	197 (RI ~40 yr.)	1:12,000 (northern portion) 1:20,000 (southern portion)	USGS
5 Aug 1992	--	--	18 Feb 1986	98 (RI ~ 9 yr.)	1:12,000	PAS
21 Mar 2000	5 Nov 1994 11 Dec1995	202 196	3 Feb 1998	165 (RI ~10 yr.)	1:20,000	PAS
Mar 2004	--	--	29 Dec 2003	91 (RI ~ 9 yr.)	1:4,800	MCDA

[a] Twenty-four-hour rainfall maximums recorded at the Kentfield rain gauge that exceed Wilson and Jayko's (1997) threshold for events capable of triggering debris flows.
[b] Peak flow totals records in Lagunitas Creek at the Samuel P. Taylor stream gauge; recurrence interval (RI) of estimated flow RI also reported.
[c] USGS: U.S. Geological Survey; PAS: Pacific Aerial Surveys; MCDA: County of Marin, Community Development Agency, GIS Division.

Field surveys were conducted to verify air photo-identified erosional scars and to identify and quantify erosional features in *ca.*64% of the catchment not amenable to air photo analysis due to dense canopy cover (see **Figure 3**). Wherever possible, estimates of erosion depth, length, and breadth were tied to age constraints, such as the apparent age of bridges and vegetation near eroding surfaces. Other recorded attributes included soil depth to bedrock and field-estimated sediment delivery to the channel network. Visual estimates of the predominance of either fine (<2 mm) versus coarse (>2 mm) sediment fraction from 212 eroding surfaces were supplemented by laboratory grain-size analysis of bulk samples taken from representative locations (n=39 hillslope and low-order tributary samples). Bulk

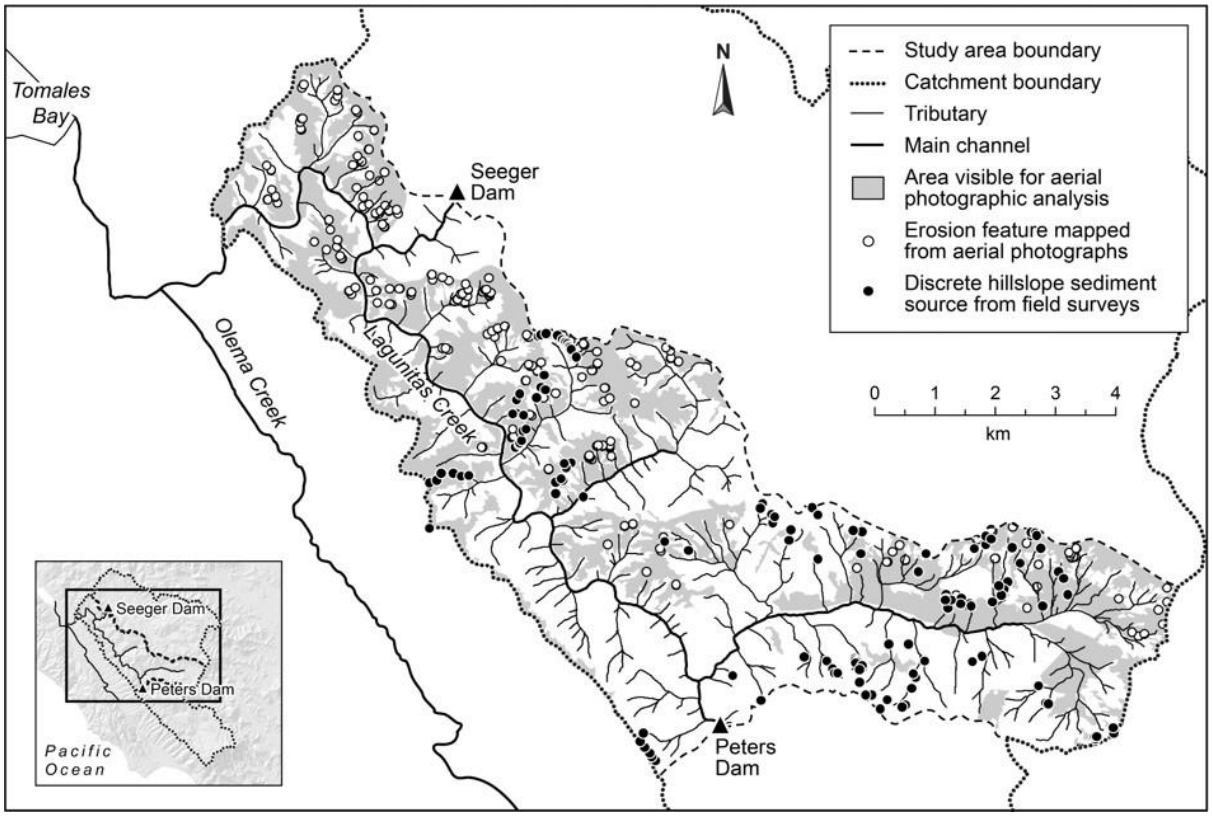

Figure 3: Hillslope sediment sources in the Middle Lagunitas Creek area identified from aerial photographic analysis (photograph dates 1982, 1992, 2000, 2004) and field surveys undertaken in 2002, 2006 and 2008.

density values for eroding surfaces of 1600 kg m^{-3} for coarse dominated ('debris flow') sediments and 1400 kg m^{-3} for fine dominated ('earth flow') sediments were utilised, based on published values from neighbouring hillslopes (Lehre, 1982; Reneau *et al*., 1984; Heimsath, 1999; Yoo, *et al*., 2005). Field estimates of length, breadth and depth of erosion features used a combination of tape survey and laser range-finder in conjunction with field experience to distinguish rupture extent from deposited volumes. Measurements were assumed to be accurate to ±0.2 m in each dimension, with evacuated material estimated as ellipsoid (landslides) or rectangular (gullies and landslide run-outs) in shape. Air-photo identified features not field-verified were estimated to be accurate to ±1 m in length and breadth, with their

volume estimated by correlation of landslide rupture area and gully rupture length to measured volumes from field-verified features (landslide $R^2 = 0.7$; gully $R^2 = 0.7$). Percentage rates of hillslope sediment delivery from landslides were derived from field estimates of the volume of the rupture scar minus the volume of downslope deposited sediment. Rates were set to zero where there was no discernible erosional path directly connecting the erosion scar to the downslope river channel. Field estimates were aggregated within individual sub-catchments to provide average values of hillslope sediment delivery.

Extrapolation of hillslope erosion process to areas under canopy and not field-accessible was based on 'geomorphic landscape units' (GLUs, Booth *et al*., 2014), a representative area approach similar to 'response units' in hydrology (Wolock *et al.*, 2004; Beighley *et al.*, 2005). Land cover, lithology and hillslope steepness were combined at the scale of their respective minimum resolution (*i.e.*, 30 m pixel size for the raster-based land cover and hillslope gradient datasets) to denote areas judged to possess similar erosion potential, and thus are functionally an extension of the 'process domain' concept (Montgomery, 1999). Sediment-production potential was extrapolated from the observed to the unobserved portion of each GLU using GIS. Similar to previous studies (*e.g.*, Reid and Dunne, 1996; Montgomery, 1999; Warrick and Mertes, 2009), hillslope GLUs combined categories of geology, land cover, and hillslope gradient. Four land management categories and four categories of geology representing broad lithological differences and were recognised to potentially influence hillslope erodibility. Three categories of hillslope steepness were defined using natural breaks in the frequency distribution of cell-based slope values (0-5%, 5-30% and >30%): such breaks are likely to separate different landform elements

284 interpreted generically here as floodplain and valley bottoms, intermediate toe and
285 hilltop slopes and steep valley sides, respectively.
286
287 **Processes of channel bed and bank erosion**
288 Channel bank erosion rates were developed from a combination of aerial
289 photographic analysis (identifying channel widening and headward channel
290 extension) and the 2002, 2006 and 2008 field surveys. Bank erosion features
291 included both chronic lateral bank retreat (recorded where >3 m^3 of material was
292 removed) and discrete mass failures which, in lower order tributaries, included failure
293 of adjacent hillslope material. The grain-size distribution of eroded material was
294 categorised visually and supplemented by laboratory particle-size analysis of bulk
295 samples collected from representative locations (n=21 mainstem bulk samples). A
296 bulk density value of 1800 kg m^{-3} for the silt-gravel-mixed bank materials were
297 utilized, based on published values from neighbouring stream channels composed of
298 similar particle-size distributions and lithologic source material (Lehre, 1982). Bank
299 erosion volumes were combined with available adjacent age constraints (*e.g.*, from
300 stratigraphic evidence, exposed tree roots, grade control structures, bridges) and the
301 estimated mean bulk density value to determine unit rates of sediment production.
302 Bank retreat estimates were obtained solely from field surveys and assumed to be
303 accurate to ±0.2 m in each of the length, height and depth dimensions, and bank
304 failures were judged to be approximately rectangular. A delivery ratio of 100% was
305 assumed based on negligible evidence for bank-derived sediment stored at the bank
306 toe.
307
308 Rates of channel bed incision rate for first- to fourth-order channels were estimated

309 using in-channel features at 46 locations and the original design drawings for one
310 bridge crossing. In the larger channels, rates were derived from nine historical
311 channel cross-section surveys, two gauging stations, and two field estimates. These
312 estimates were combined with a representative channel width (according to stream
313 order), channel length and sediment bulk density (2,000 kg m^{-3}; Lehre, 1982) to
314 determine average unit rates for either incision or aggradation. The average depth
315 of incision derived from cross-section survey data was assumed to be accurate to
316 ±0.02 m and the representative channel width to ±1 m. Rates of incision were
317 extrapolated uniformly between cross-section surveys.
318
319 Extrapolation of average unit bank erosion and bed incision rates to unsurveyed low
320 order channels was achieved by defining a 'channel GLU' based on underlying land
321 use and geology categories to characterize the channel's riparian setting, and use of
322 Strahler stream order (Strahler, 1952) to systematically distinguish channel
323 segments that exhibit unique gradient and geometric qualities (see Table 2b). Rates
324 of bank erosion in higher order channels were age-constrained directly using
325 channel topographic survey data or by estimating erosion around young, dated, tree
326 species, or erosion past established older trees (assuming erosion occurred since
327 1982). Rates with the latter technique are highly approximate and assumed
328 accurate to ±5 years based on analysis of six tree cores collected from San
329 Geronimo Creek, Devils Gulch, and mainstem Lagunitas Creek.
330
331 **Non-point hillslope sources**
332 Diffuse processes of hillslope sediment production, such as soil creep, are non-linear
333 and slope-dependent (Roering *et al.*, 1999, 2001) and thus very difficult to observe.

334 Consequently, we applied a numerical soil production and diffusion model developed
335 for the region (see Dietrich *et al.*, 2003). Production rates were determined as an
336 inverse exponential function of soil depth calibrated against a maximum inferred
337 long-term soil erosion depth of 268 m Ma^{-1} using evidence from cosmogenic nuclide
338 decay in nearby Tennessee Valley (Heimsath *et al.*, 1999). After simulating initial
339 conditions, average yearly flux rates for the period WY 1983–2008 were estimated
340 using a diffusion function set to 45 cm^2 a^{-1} based on published values from a
341 neighbouring catchment exhibiting similar physical attributes (Dietrich *et al.*, 1995);
342 soil reaching the channel is routed from the system.
343
344 **Erosion processes connected with roads and trails**
345 Sediment erosion from roads and trails, which can be highly significant when
346 unpaved roads are subject to heavy use (*e.g.*, Wemple *et al.*, 2001; MacDonald *et*
347 *al.*, 2001; Croke *et al.*, 2006), was derived using a GIS-based road erosion and
348 delivery model (SEDMODL2: NCASI, 2005). The model identifies road segments
349 with high potential for sediment delivery to stream networks as a function of distance
350 to stream crossings and so rates vary considerably according to the density of
351 stream crossings. The model is based on various factors superimposed over a
352 USGS 10-m digital elevation model (DEM) including geology, soils, average annual
353 precipitation, vegetation cover and attributes of road type, surface type, width, and
354 age.
355
356 **Assessing Uncertainties**
357 The variety and disparate nature of data sources used to construct a catchment
358 sediment budget means that they are rarely amenable to a formal error analysis

(Evans and Warburton, 2005; Hinderer, 2012; Reid and Dunne, 1996, 2016). Further, in decadal-scale budgets, the necessary use of historical data sources introduces various data measurement and interpretation errors that cannot be addressed directly. Here, the procedure for assessing uncertainties and minimizing errors is based on three complementary approaches that check on both accuracy and precision.

The first assurance on accuracy involves deriving rates for each of the dominant sediment processes in the host geomorphic province and to estimate all elements independently, to avoid representing processes through unmeasured residuals (Kondolf and Matthews, 1991). Second, the accuracy of average sediment yield estimates was corroborated using independent data derived from sediment gauging records and bathymetric surveys of reservoir sedimentation, as detailed below, and against sub-catchment sediment yield estimates reported from neighbouring catchments. Third, *precision* was assessed by estimating measurement errors for the various sediment processes, and propagating these errors in quadrature (Taylor, 1997). The principal sources of error inherent to each component of the budget was determined based on field experience (measured dimensions and age estimates), reported ranges of variability (bulk densities), standard errors of the mean (area to volume conversion for landslide depth, suspended sediment rating curve) and sensitivity testing (numerical models).

Sediment discharge data from three streamflow gauging stations in the catchment (see Figure 1) provided point sediment yields for corroborating with extrapolated field survey results. Each gauge has been periodically sampled for suspended sediment

384 during the study period, with bedload samples also collected at the San Geronimo
385 Creek (SGC) gauge using a Helley-Smith portable sampler (Owens *et al*., 2007) with
386 collection periods and techniques varying between each gauge. Suspended
387 sediment rating curves were developed for each gauge using a locally-weighted
388 scatterplot smoothing function (LOWESS, Cleveland, 1979) that generates a
389 weighted least-squares regression curve that is little affected by 'outlier' data (Hicks
390 *et al.*, 2000; Warrick *et al.*, 2004). Combining suspended sediment load and bedload
391 data at the SGC gauge between 1982 and 2008 showed bedload to represent 31%
392 of the total sediment load. This value is high (*cf*. Slagel and Griggs, 2008) and may
393 reflect the significant component of fine bed material (1–4 mm) observed in bed
394 sediments. Based on this value, and a presumed downstream reduction in fractional
395 bedload transport, bedload through the SPT and PRS gauges was set at 15%. The
396 suspended sediment and bedload discharge rating curves for each gauge were
397 combined with daily mean flow data to develop estimates of average annual
398 sediment yield.
399
400 Corroboration via bathymetry was achieved by comparing estimated reservoir
401 sedimentation rates for two upstream arms of Nicasio Reservoir (see Figure 1) to an
402 uncalibrated, GLU-based extrapolation of sediment yield from the contributing
403 Nicasio Creek catchment area. Bathymetric surveys of reservoir infilling (2008) were
404 derived from Acoustic Doppler Current Profiler (ADCP) surveys compared to multiple
405 cross-sections from 1976 (post-reservoir) and a pre-reservoir topographic map from
406 1961, with extrapolation between cross-sections to estimate deposited sediment
407 volumes based on recommendations in Juracek (2006). Volume-to-mass conversion
408 is subject to the inherent highly variable nature of bulk density of reservoir

409 sediments, related primarily to sediment source lithology and the position of the
410 sample in the reservoir: a value of 1.4 tm^{-3} was chosen based on published values
411 (Murthy, 1977; Snyder *et al*., 2004; Juracek, 2006; Minear and Kondolf, 2009).
412 Corroboration is thus highly approximate according to assumed bulk density,
413 variable survey resolutions and because the surveys bracket different time periods
414 with a different distribution of sediment-generating events.
415

416 # 4. RESULTS

417 **Catchment and Channel Character**

418 The GLUs provide a basis for extrapolating results but also a succinct summary of
419 potential hillslope erodibility. Area data in **Table 2a** indicates that the Middle
420 Lagunitas Creek study area has very similar attributes to the overall Lagunitas
421 catchment, with high potential erodibility, resulting from a preponderance of steep
422 slopes (>30%) and erodible sediments (Franciscan mélange), possibly mediated by
423 a significant proportion of 'mixed forest' land cover. Combined into GLUs, 21 out of
424 48 possible permutations cover 1% or more by area, cumulatively totalling 93% of
425 the Lagunitas catchment area. The numerical codes used to denote each GLU are
426 explained in Table 2 and Figure 5. In Middle Lagunitas Creek just eight GLUs cover
427 79% of the total area (see **Figure 4**) with the most prevalent GLU combining dense
428 forest, Franciscan mélange lithology, and steep slopes (GLU 243: 19% of study
429 area). The second most common GLU has dense forest and Nicasio Reservoir
430 terrain on steep slopes (GLU 223: 11.5% area), and the third combines dense forest
431 and Franciscan mélange on moderate slopes (242: 8.5% area). Areas of agricultural
432 grasslands are next, situated on Franciscan mélange with moderate or steep slopes
433 (GLUs 142, 143), thus combining highly erodible terrain with significant land

434 disturbance.

435

Table 2a - Summary character of Lagunitas Creek catchment expressed in terms of Geomorphic Landscape Unit attributes of land cover, geologic terrain and hillslope gradients. Values for study area in bold font.

Geomorphic Landscape Unit Attribute	Code	Lagunitas Cr. above Peters Dam (55.7 km^2)	Middle Lagunitas Creek (64.4 km^2)	Nicasio Cr. Above Seeger Dam (93.2 km^2)	Total catchment (213.2km^2)
			Percent cover		
Land cover (first digit)					
Agricultural/Herbaceous	1	8	**32**	56	36
Mixed Forest >50% canopy	2	51	**53**	32	43
Mixed Shrub <50% canopy	3	35	**13**	9	17
Urban/Barren surfaces	4	7	**2**	4	4
Geologic terrain (second digit)					
Quaternary alluvium	1	6	**4**	5	5
Nicasio Reservoir	2	24	**24**	4	16
San Bruno Mountain	3	8	**16**	16	14
Franciscan mélange	4	57	**56**	70	63
Hillslope gradient (third digit)					
0–5%	1	6	**4**	9	7
5–30%	2	28	**35**	38	35
>30%	3	66	**61**	53	59

Example: GLU code 343 represents a geomorphic landscape unit with shrub/forest with less than 50% canopy cover underlain by Franciscan mélange on slopes greater than 30%

436

Table 2b - Summary character of Lagunitas Creek river channels expressed as attributes of Strahler stream order. Channel gradients could not be surveyed directly in the sixth-order channels and are assumed equal to those in the fifth-order channels.

Order	Channel length (m)	Average channel width (m)	Mean channel gradient (± 1 std. dev.)
1	108,000	0.6	0.196 (± 0.101)
2	36,000	1.2	0.116 (± 0.074)
3	11,300	2.7	0.024 (± 0.009)
4	8,700	10	0.009 (± 0.006)
5	12,600	12	0.005 (± 0.002)
6	4,350	15	0.005 (± 0.002)

437

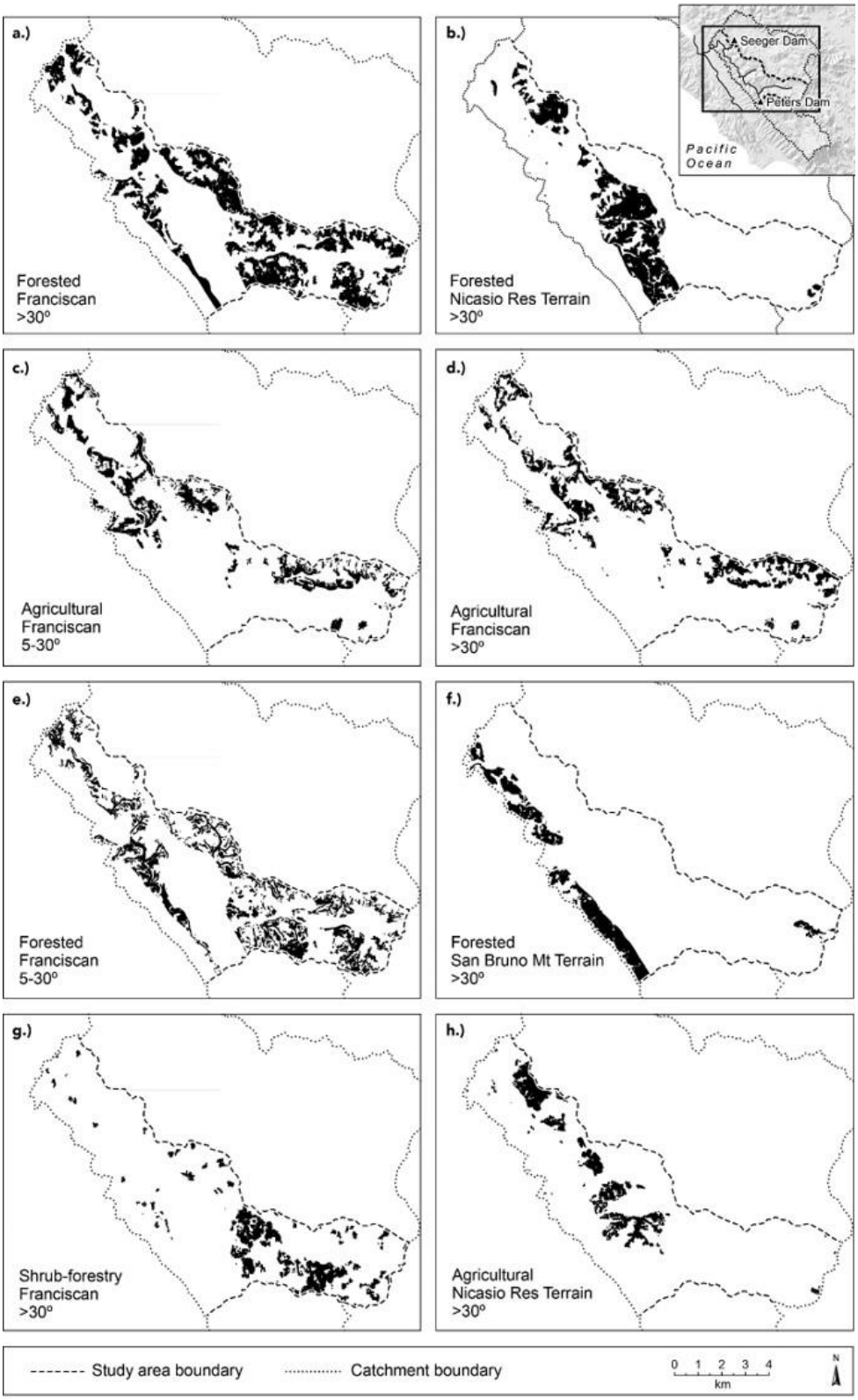

438

439 Figure 4: Example of Geomorphic Landscape Units (GLUs, Booth *et al.*, 2014) for
440 the Middle Lagunitas Creek area. The GLUs provide the basis for
441 extrapolating field survey observations to the study area. Illustrated here
442 are eight GLUs that cover 79% of the area (see Table 4). The remaining
443 40 combinations (not depicted) cover the remaining 21%.

444 Channel width and gradient were clearly distinguished by Strahler stream order as
445 channels transform from steep headwater 'colluvial' type tributaries to pool-riffle type
446 mainstem channels (Montgomery and Buffington, 1997 classification) (**Table 2b**).
447 Eight combinations of riparian land use and geology were frequently associated with
448 bank erosion processes (see results below), including sites on Quaternary alluvium
449 and bordered by urban land uses, reflecting erosion stemming from local
450 development pressures on floodplains.
451
452 **Sediment Production and Delivery Processes**
453 Hillslope surveys accessed GLUs representing ~50% of the study area (32.3 of 64.4
454 km^2; **Table 3**) with examination of aerial photographs capturing the remainder of
455 area without canopy cover. Channel surveys encompassed a stratified sample of
456 first- to fourth- order tributary channels and nearly all of the higher order Lagunitas
457 and San Geronimo creeks. Hillslope processes were dominated by gully and rill
458 erosion (59 of 115 discrete sources) and shallow landslides (n=47) but the few deep-
459 seated landslides (n=9) were volumetrically larger leading to an almost equal
460 contribution to volumetric sediment production (31%, 35%, 34%, respectively). Field
461 evidence suggested that, volumetrically, an average of two-thirds of the eroded
462 hillslope sediment was delivered to the channel network, with a range that varied
463 from 34% to 81% in the 68 individual sub-catchments. The <2 mm sediment
464 component of field samples ranged from 14% to 95% but at a sub-catchment level
465 consistently averaged 50-60% of sediment and is thus proportional to overall rates of
466 hillslope erosion.
467
468 Hillslope sediment production (**Figure 5a**) and delivery (**5b**) from deep-seated

469 landslides is concentrated in mixed shrub landscapes whereas shallow landslides
470 are proportionately far more common in agricultural areas. Erosion rates are
471 generally smaller under mixed forest but greatest on Franciscan mélange sediments
472 because all observed deep-seated landslides are associated with this lithology
473 (**Figure 5c, d**). Unsurprisingly, erosion rates are also greatest on the steepest
474 hillslopes; moderate slopes permit delivery from gullies and rills as effectively as
475 from steeper slopes but are apparently ineffective at delivering material from shallow
476 landslides which is instead re-deposited downslope and does not reach the channel
477 (**Figure 5e, f**). Combined as GLUs, the results indicate that rates of hillslope
478 sediment production are maximised on steep slopes on Franciscan mélange with
479 shrub vegetation because deep-seated landslides are focused here (GLU 343,
480 **Figure 5g**); however, steeply-sloping Franciscan mélange with agricultural grazing
481 has almost comparable rates of landslide delivery overall due to effective delivery of
482 shallow failures (GLU 143, **Figure 5h**). Overall, sediment production from discrete-
483 source hillslope processes in Middle Lagunitas Creek amounts to ~8,000 t a^{-1}
484 (equivalent unit area rate of ~120 t km^{-2} a^{-1}, **Table 3**), ~69% of which is derived from
485 shallow- and deep-seated landslides, the remaining 31% from gullies and rills.
486 Uncertainties in data generation for discrete hillslope sources result in a high
487 estimated error (± 73% see section below). Approximately 54% of this production
488 (4,300 t a^{-1}) is estimated to comprise sand or finer grain sizes.
489

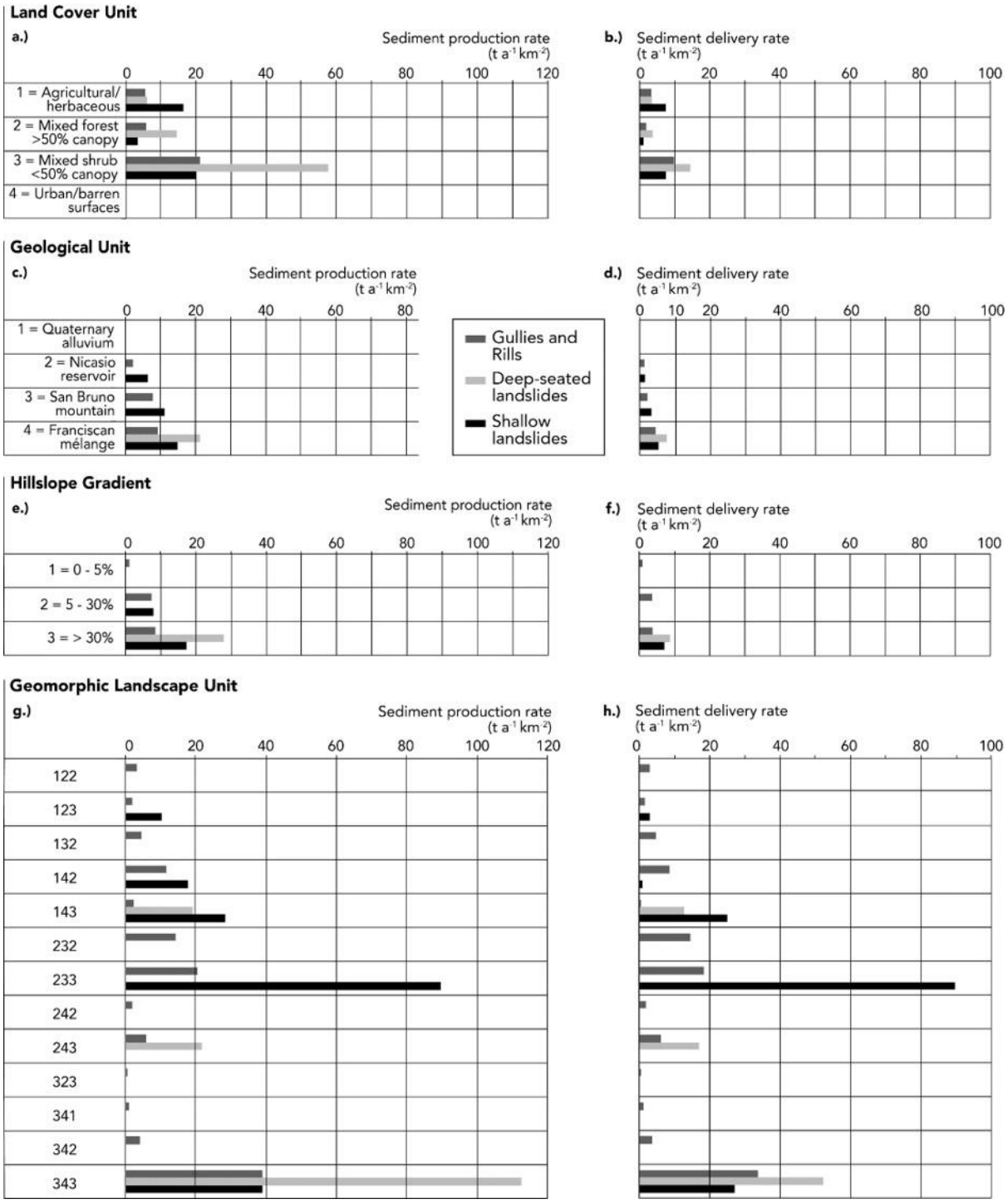

Figure 5: Area-normalized hillslope sediment production and delivery rate (t a^{-1} km^{-2}) for surveyed study area land cover (a = production, b = delivery), geology (c, d), hillslope gradient (e, f) and combined as GLUs (g, h).

Table 3 - Summary of hillslope sediment production for the Lagunitas study area as extrapolated from sampled GLUs using field surveys (2002, 2006, 2008) and aerial photographic analysis of erosion features.

Sampled GLUs	Sampled area (km^2)	Total eroded mass [a] (t)	Sediment production rate of sample GLU (t km^{-2})	Extrapolated to Middle Lagunitas (effective sediment producing area) [64.4 km^2]		
				GLU total area (km^2)	Extrapolated eroded mass (t)	Extrapolated GLU sediment production rate: WY1982-2008 (t a^{-1})
111	0.5	1,610	3,000	0.6	1,690	65
112	0.6	360	580	0.7	400	15
122	1.2	3,000	2,560	1.3	3,420	132
123	2.8	19,550	7,050	3.6	25,230	970
132	1.8	840	475	2.0	950	36
133	0.7	2,520	3,610	0.8	2,910	112
142	5.0	22,380	4,500	5.5	24,820	955
143	4.9	50,360	10,340	5.5	56,720	2,180
222	0.3	120	410	1.6	670	26
223	2.7	2,460	930	7.4	6,860	264
232	0.3	330	1,200	2.0	2,430	93
233	0.3	1,700	4,920	4.3	21,070	810
242	2.2	1,710	770	5.6	4,300	165
243	5.3	11,600	2,190	12.2	26,620	1,020
323	0.6	6,740	12,130	1.2	14,940	575
342	0.9	2,610	2,900	2.1	6,180	238
343	2.1	4,210	1,980	3.8	7,550	290
411	0.3	0	10	0.4	0	0
Total	**32.3**	132,100	4,090	**60.6**	206,800	7,950
Average annual production rate (t km^{-2} a^{-1})						**124**

[a] Overlapping sediment source sites from the four surveys were reconciled to avoid double-counting sites. Overlap determined using a 15 m buffer around the digital data points (field survey sites), lines (air photo mapped gully sites), and areas (air photo mapped landslide sites) in GIS. The sum of terrain mass is derived by addition of non-overlapping hillslope sediment source sites; mass yield assume bulk density values ranging from 1.4 to 1.6 t m^{-3}

In-channel sediment production is widespread through the study area with discrete bank erosion surveyed at 389 sites which, when extrapolated, is estimated to contribute ~5,350 t of sediment annually. Erosion sources were maximised in first-order tributaries and mainstem channels of fourth-order (**Figure 6a).** Smaller failures were common in low-order channels and occurred most frequently in the very common mixed forest and Franciscan mélange riparian setting (125 failures surveyed, **Figure 6b**). These failures are presumed to partially reflect headward extension of the drainage network resulting from hillslope disturbances. Larger failures are proportionately more frequent in the higher-order mainstem channels, with 55% of failures producing a yield equivalent to > 2.5 t a^{-1} (**Figure 6a)**. They are thus associated with shrub-forested Franciscan mélange on alluvial floodplains and are assumed to result from incision downstream of the two major dams. Unit rates of average bank erosion ranged over two orders of magnitude (<0.001 to 0.166 t m^{-1} a^{-1}) with the highest overall unit rate occurring in a short stretch of Lagunitas Creek immediately downstream of the confluence with regulated Nicasio Creek. Bank erosion rates in first-order tributary channels were highest on Franciscan mélange bordered by shrub-forest land cover (0.108 t m^{-1} a^{-1}) in part to its ubiquity, but rates are highest in second order channels on Franciscan mélange that drain urban areas (0.139 t m^{-1} a^{-1}).

Channel bed erosion was also pervasive through the study area. Averaged incision rate estimates in the first-to-third order tributaries ranged from 0.006 to 0.035 m a^{-1} with values stratified and extrapolated to unsurveyed channels via channel GLUs. The largest proportion of tributary channels were in forested Franciscan mélange

settings (36, 42, 49%, respectively) and had incision rates of 0.018, 0.006 and 0.012 m a^{-1}, respectively, thus heavily influencing order-averaged incision rates of 0.014, 0.008 and 0.011 m a^{-1}. Incision estimates for fourth-to-sixth order channels indicated rates of erosion varying from 0.006 to 0.018 m a^{-1}. The maximum rate occurred just below the San Geronimo Creek-Lagunitas Creek confluence and may reflect prograding incision downstream from Peters Dam located on Lagunitas Creek approximately 0.7 km upstream of the confluence. A 6-km aggrading channel reach occurs further downstream on Lagunitas Creek and above the confluence of the regulated Nicasio Creek (below which incision re-commences).

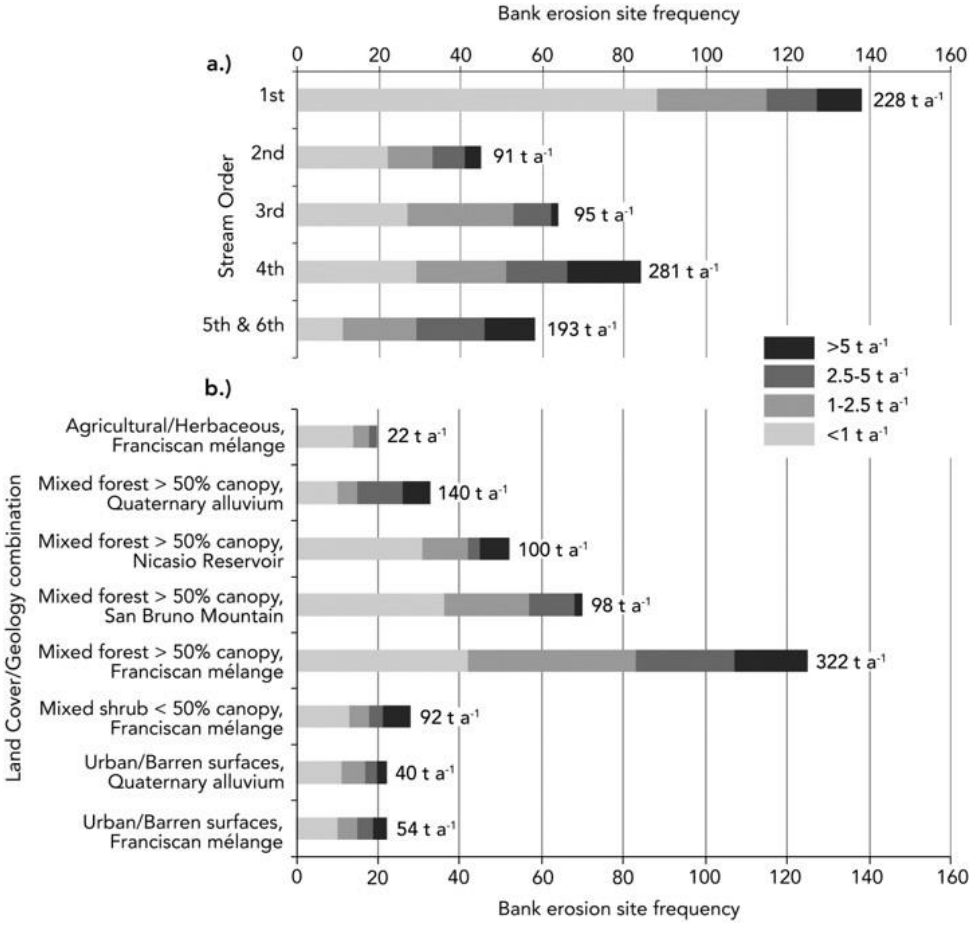

Figure 6: Results from surveys of 389 bank erosion sites sub-divided by (a) stream order and bank failure size, (b) land cover / geological terrain and bank failure size.

Modelled rates of soil production and diffusion varied from approximately 3.3 to 5.8 t km^{-2} a^{-1} by sub-catchment, consistent with field monitoring of a neighbouring catchment of similar topography, geology and land cover (Lehre, 1982) with soil creep estimates of 2 to 7 t km^2 a^{-1}. Sub-catchment-based sediment yields from road-related erosion processes were predicted by use of SEDMODL2 to range from ~2 t km^2 a^{-1} to a maximum of 65 t km^2 a^{-1} in San Geronimo Creek which has the greatest density of unpaved roads.

Uncertainty analyses focused on estimating the precision in individual process estimates through error propagation and corroborating the accuracy of average sediment yield estimates against independent data. With regards to precision, the primary hillslope and channel process estimates are products of components representing dimensions, shape, delivery ratio, mass conversion and process rate annualisation, with various sources of error and assumptions relating to each component (see **Table 4**). Errors related to each component are assumed to be independent, allowing their combination as a product in quadrature (Taylor, 1997), a process that produces an overall error somewhat in excess of the largest individual component error. Product errors here are mostly in excess of 50% (range 36–91%), with the largest error sources generally related to derived average values, notably the area-to-volume conversion factor associated with hillslope slides and gullies (80%). The error associated with each of the modelled components was unknown and instead the outputs were subject to sensitivity testing to bound the likely range of results. As each is a reasonably small part of the sediment budget, this error has limited influence on the average annual sediment yields. Errors associated with the overall average annual sediment delivery were combined as a sum in quadrature

(Taylor, 1997).

The largest error associated with the corroborating estimates for reservoir sedimentation results from the application of the coarse 10 ft. contour (in native measurement) topographic maps (1961) to derive pre-reservoir baseline conditions. This is largely responsible for the combined 54% error estimate (**Table 4**). The broad prediction intervals associated with each LOWESS-fitted sediment rating curve (example as **Figure 7**) occurs in part due to the combination of ENSO-driven climate variability and presence of large dams. Together, they impart a 'binary' flow and sediment response between years typified by regulated low flows and those including 'unregulated' high flows (every 5–8 years) and thus annual sediment yields are highly variable (see Discussion).

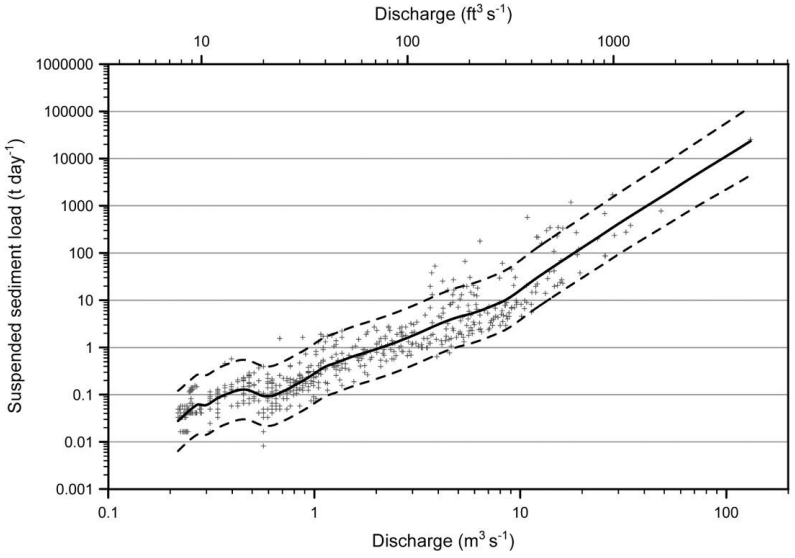

Figure 7: Suspended sediment rating curve for the Samuel P. Taylor State Park (SPT) gauging station. The rating curve is based instantaneous discharge and corresponding instantaneous readings by a calibrated OBS sensor WY2004–2006 which are then converted to sediment discharge values and scaled to tons/day by the USGS (for method see Curtis, 2007). Locally-Weighted Scatterplot Smoothing (LOWESS), after Cleveland (1979) was employed with a bandwidth of 0.2 (percentage of points included in each of the local regression iterations) and 95% global prediction intervals applied following the method of Loader (1999, p.30).

589 **Average Annual Sediment Yield**

590 Following extrapolation to unsurveyed areas, total net sediment yield from Middle
591 Lagunitas Creek is estimated to average ~20,000 t a^{-1} ± 6,000 t a^{-1} for the period
592 1983–2008 (**Table 5**), equivalent to ~300 t km^{-2} a^{-1} from the effective sediment-
593 producing area downstream of major dams. The average unit yield for the 67 sub-
594 catchments is ~200 t km^{-2} a^{-1} with a standard deviation of ~100 t km^{-2} a^{-1}.

595

596 Hillslope slides and gullies account for 26% of all sediment delivered, which is
597 slightly less than from channel bank erosion sources (29%), and less still than
598 sediment emanating from channel incision (33%), results that are perhaps logical for
599 a highly regulated catchment. Whereas incision-derived sediment derives almost
600 equally from tributary and mainstem sources, the vast majority of bank erosion
601 originates from low-order tributary sources. Modelled rates of sediment delivery from
602 soil creep and from roads and trails provides a reasonably small sediment
603 contribution overall (1% and 10%, respectively) but, locally, roads and trails may
604 represent the sources of nearly 17% of all sediment delivered in the San Geronimo
605 Creek catchment. San Geronimo Creek also accounts for nearly one-half (46%) of
606 the total sediment delivery from 38% of the study area (385 t km^{-2} a^{-1}), a yield that is
607 exceeded only by the short, incising section of Nicasio Creek downstream of Seeger
608 Dam (~500 t km^{-2} a^{-1}). The lowest unit rate of sediment delivery occurs in the
609 Lagunitas Creek mainstem from the Devils Gulch to Nicasio Creek confluences
610 where sediment storage through aggradation reduces the effective unit yield from
611 214 t km^{-2} a^{-1} to 133 t km^{-2} a^{-1}, despite this unit having the highest unit rate of
612 hillslope sediment delivery (96 t km^{-2} a^{-1}).

613

614 **Table 4 – Component-based error estimates and propagated total error for the various processes represented herein. L= length, w = width, d =**
615 **depth**
616

Process Estimate	Components	Primary sources of error	Error assumptions	Estimated error
Field estimated hillslope slides and gullies	Dimensions (l, w, d)	Field measurement errors	± 0.2 m each dimension, applied to field samples	± 21%
	Shape	Ellipsoid for landslides, rectangles for gullies	Assume compensation between samples	-
	Delivery ratio	Field estimate of proportion delivered	Standard deviation of mean delivery ratio	± 38%
	Mass conversion	Field estimated bulk density estimate	1.5 t kg^{-3} ± 0.2 t kg^{-3}	± 13%
	Annual rate	Data available for age constraint – storm records, air photos	Average of *ca.*2 years between air photos and storms and/or survey	± 8%
			ERROR ESTIMATE	± 46%
Air photo estimated hillslope slides and gullies	Dimensions (l, w)	Digitising aerial photographs	± 1 m each dimension, applied to identified failures (average 191 m^2)	± 12%
	Dimension (d)	Area to volume conversion, based on regression from field samples	Standard error	± 80%
	Shape	Ellipsoid for landslides, rectangles for gullies	Assume compensation between samples	-
	Delivery ratio	As estimate from field data	Standard deviation of mean delivery ratio	± 38%
	Mass conversion	As estimate from field data	1.5 t kg^{-3} ± 0.2 t kg^{-3}	± 13%
	Annual rate	Data available for age constraint – storm records, air photos	Average of *ca.*2 years between air photos and storms and/or survey	± 8%
			ERROR ESTIMATE	± 91%
All hillslope		**Air photo failure mass = 61% of total**	**HILLSLOPE PROPORTIONAL ERROR**	**± 73.3%**
Channel bank erosion	Dimensions (l, w, average d)	Field measurement errors	± 0.2 m l, w; 25% d (0.8m average)	± 26%
	Shape	Cubic block on average d	Assume compensation between samples	-
	Delivery ratio	Field estimate of proportion delivered	All sediment delivered to channel	-
	Mass conversion	Bulk density, from literature	1.8 t kg^{-3} ± 0.2 t kg^{-3}	± 11%
	Annual rate	Data available for age constraint – infrastructure records, tree rings	± 5 years based on sample cores	± 19%
			ERROR ESTIMATE	**± 36%**
Channel bed erosion	Dimension (w)	Stream order-averaged width, based on field estimates and surveyed cross-sections	Average value of measurement error by stream order	± 12%
	Dimension (d change)	Field estimates and measurement error where cross-section surveys (mainstem)	Average of ± 0.02 m from repeat cross-sections (n=11); 50% where field estimated (n=48)	± 44%

	Dimension (l)	From field surveys and air photos	Length estimate negligible component of error; assumes consistent w, d between cross-sections	-
	Bulk density	Mass conversion	2.0 t kg^{-3} ± 0.2 t kg^{-3}	± 10%
	Annual rate	Data available for age constraint – infrastructure records, surveyed cross-sections	Judgment based on highly-constrained ages where repeat surveys (25% of sample set) and poorly constrained otherwise.	± 25%
			ERROR ESTIMATE	**± 54%**
Creep and biogenic transport	Calculated yield	Model input data, yield algorithm	Error unknown – very minor component of sediment budget.	**± 50%**
Road and trail erosion	Calculated yield	Model input data, yield algorithm	Error unknown – minor component of sediment budget	**± 50%**
Reservoir sedimentation	Dimensions (d)	Interpolation between surveyed cross-sections from 1976 (post-reservoir), mapped contours from 1961 pre-reservoir topographic maps, and 2008 bathymetric surveys using ADCP.	Pre: all measurements ± 5 ft. (native measurement) Post: assume 0.01 m resolution (manufacturer claims) – negligible error impact	± 50%
	Dimensions (w, 1)	As above	± 1 m for each, on cross-sections averaging a width of 150 m	± 1%
	Bulk density	Mass conversion, based on literature estimates of reservoir sedimentation density	1.4 t kg^{-3} ± 0.3 t kg^{-3}	21%
	Annual rate	Sedimentation extends over period of record longer than sediment budget period	Assumed representativeness	-
			ERROR ESTIMATE	**± 54%**

617
618
619

Table 5 - Annual rates of sediment delivery estimated for major sub-divisions of the Middle Lagunitas Creek area

Unit	Drainage area (km^2)	Sediment delivery ($t\ a^{-1}$)					Sediment yield ($t\ a^{-1}$)
		Hillslope slides and gullies	Soil creep	Roads and trails	Channel bank erosion	Channel bed incision	Unit total
San Geronimo Creek	24.3	1,840	90	1570	3000	2860	9,360
Lagunitas Creek (San Geronimo Creek to Devils Gulch)	8.8	700	50	230	510	1570	3,060
Devils Gulch	7.0	520	30	60	590	670	1,880
Lagunitas Creek (Devils Gulch to Nicasio Creek)	14.9	1,430	60	10	1100	-640	1,980
Regulated Nicasio Creek	2.3	180	10	0	40	920	1,140
Lagunitas Creek (Nicasio Creek to Pt. Reyes Station)	7.1	650	30	160	580	1300	2,720
	Propagated error	73%	50%	50%	36%	54%	28.8%
Total study area	**64.4**	**5,330 ± 3,910**	**270 ± 1350**	**2,040 ± 1,020**	**5,820 ± 2,090**	**6,680 ± 3,600**	**20,135 ± 5,800**

Table 6 – Comparison of sediment delivery and yield information from extrapolated field surveys, gauging station data and bathymetric survey.

Sub-catchment area	Effective drainage area	Sediment yield from gauged data WY 1983–2008	Unit rate	Sediment yield from reservoir sedimentation WY 1961–2008 [c] WY 1961–1976 [d]	Unit rate	Sediment delivery from GLU-extrapolated field surveys WY 1983–2008	Unit rate	Percentage difference using GLU estimate
	km^2	$t\ a^{-1}$	$t\ km^{-2}\ a^{-1}$	$t\ a^{-1}$	$t\ km^{-2}\ a^{-1}$	$t\ a^{-1}$	$t\ km^{-2}\ a^{-1}$	
San Geronimo Creek (SGC) at Lagunitas Road bridge	23.1	5,250 ± 7,700	227 ± 330	n/a	--	8,850 ± 2,550	383 ± 110	**+69**
Lagunitas Creek at Samuel P. Taylor State Park (SPT)	32.7[a]	4,270[c] ± 7,500	130 ± 230	n/a	--	12,330 ± 3,550	377 ± 109	**+190**
Lagunitas Creek at Pt. Reyes Station (PRS)	62.4[b]	17,400[c] ± 19,400	279 ± 310	n/a	--	19,700 ± 5,670	316 ± 91	**+13**
Nicasio/Halleck Creek arm	54.9	n/a	--	25,480 [d] ± 13,760	464 ± 250	17,550 ± 5,050	320 ± 92	**-31**
Nicasio Reservoir (u/s of Seeger Dam)	93.2	n/a	--	32,640 [e] ± 17,630	350 ± 189	26,600 ± 7,660	285 ± 82	**-19**

[a] 63% of 88.8km^2 is regulated

[b] 71% of 211.6 km^2 is regulated

[c] Bedload is assumed to be 15% of the suspended load

Delivery rates predicted from extrapolated field data exceeds yields obtained from sediment gauging data but is less than bathymetry-based yield estimates (**Table 6**). The estimates are most comparable for larger catchment areas (extrapolated yield is only 13% higher than the Point Reyes Station (PRS) gauging station estimate, and 19% less than the full Nicasio reservoir estimate), perhaps hinting at an inherently conservative extrapolation process. This mechanism may also be responsible for the greatest deviation from gauged data, which occurs at the SPT gauge: this gauge is located a short distance downstream of Peters Dam which must very effectively regulate suspended sediment – a local factor that is not accommodated in the areal extrapolation process.

Average annual sediment budget WY 1983–2008

Figure 8 depicts the decadal-scale sediment budget for Lagunitas Creek catchment. The average annual catchment yield of just over 20,000 ± 6,000 t a^{-1} is comparable to the transport load estimated to pass through the downstream-most gauging station (PRS) of ~17,000 ± 19,000 t a^{-1} (**Table 6**). Middle Lagunitas Creek has been characterized since WY 1983 by sediment export (84% of the ~24,000 t a^{-1} produced) rather than sediment storage (~4,000 t a^{-1}), with much of the exported sediment obtained from alluvial sediment stores subject to processes of mainstem and tributary incision and associated bank failures. Channel-derived sediments account for nearly 57% of the total yield, greatly exceeding the proportion delivered from hillslope sources (34% from hillslope slides, gullies, and soil creep; **Figure 9**).

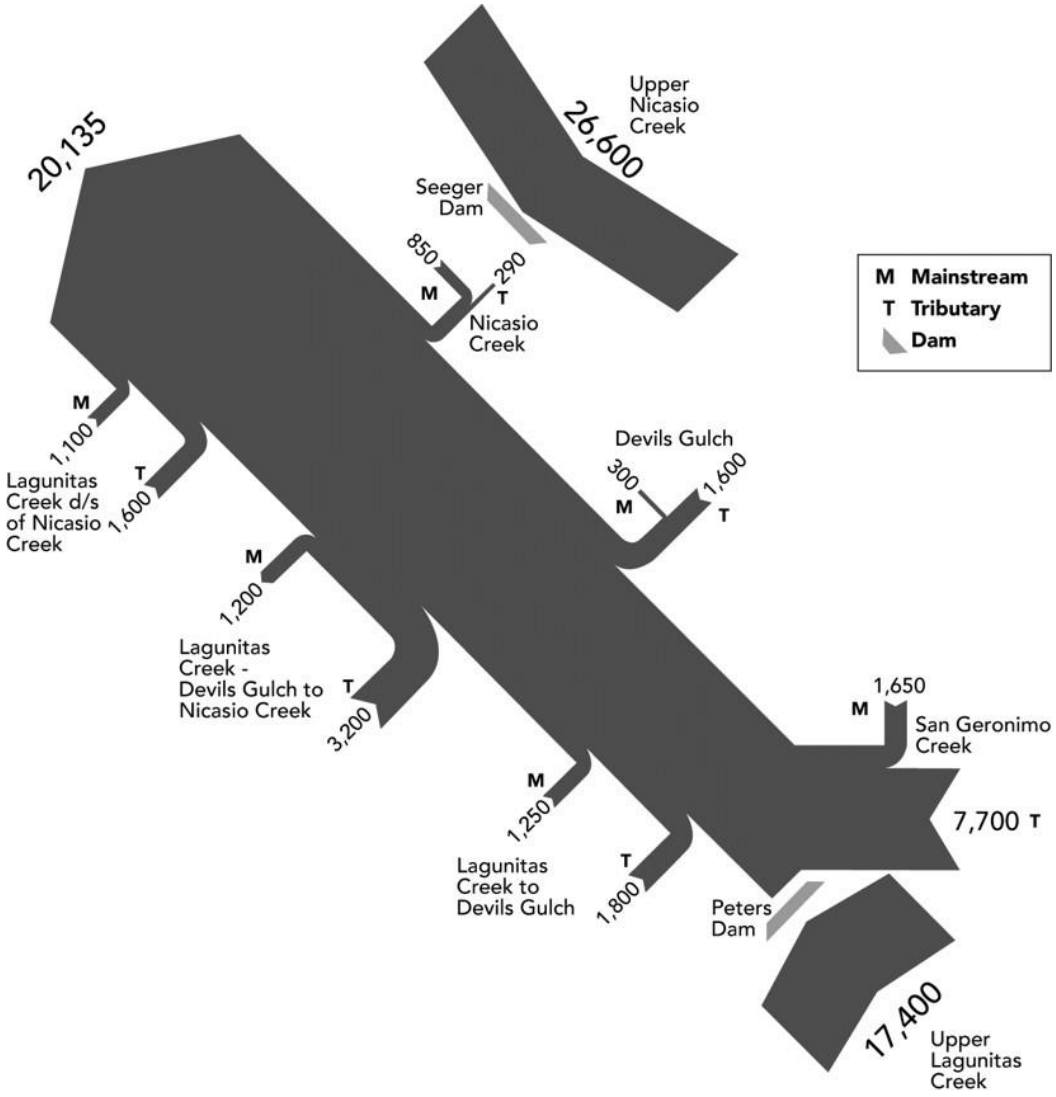

Figure 8: Contemporary (1983-2008) average annual sediment budget for Lagunitas Creek catchment, including estimates of disconnected sediment delivery upstream of major dams. Sediment volumes in t a^{-1}. Separate values are provided for the loads generated by processes directly associated with the mainstem river (M: Lagunitas Creek, San Geronimo Creek, Nicasio Creek, Devils Gulch) and from the tributaries and their associated hillslopes (T). Note that aggradation in the mainstem reach of Lagunitas Creek from Devils Gulch to Nicasio Creek results in the only network loss of sediment (*cf.* for instance, Trimble 1999) Estimates for those areas upstream of large dams are based on extrapolated GLUs (*i.e.*, without field calibration) and modelled soil creep and road-related sediment production.

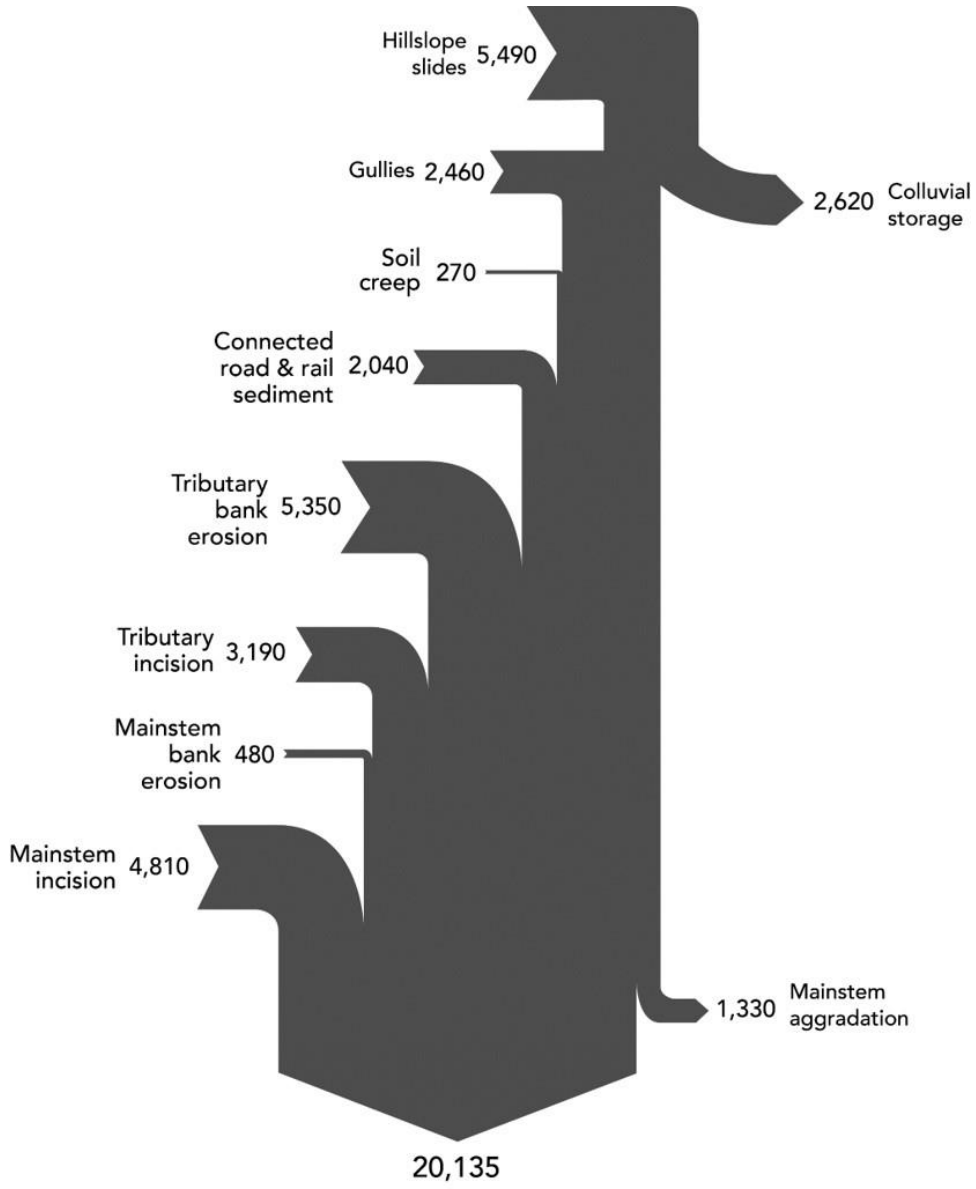

Figure 9: Process-based sediment budget (1983-2008) for the Middle Lagunitas Creek study area. Sediment volumes in t a^{-1}.

5. DISCUSSION

Previous sections have described an approach for constructing a distributed, process-based sediment budget for a catchment whose size dictates that process rate estimates are necessarily derived from direct and secondary data, models and

extrapolation, rather than from direct monitoring. Individual estimates were subjected to independent corroborative checks on their gross accuracy, and the precision of the resulting budget evaluated via an uncertainty assessment that is perhaps unique to a catchment of its size (i.e., >10 km^2). The utility of this approach to sediment budgeting is evaluated below, focusing on the insights achieved in terms of recent changes in fluvial system dynamics and the value and apparent implications of the uncertainty assessment. To begin, the budget is placed in its spatio-temporal geomorphological context.

Temporal and spatial context and corroboration

The contemporary unit yield from the Middle Lagunitas Creek area (64 km^2), estimated from field survey, supplemented by air photo analysis and extrapolated by GLU, is 315 ± 90 t km^{-2} a^{-1} (see **Table 5**). The value is similar to maximum historical rates of sedimentation reported at the catchment mouth of 325 t km^{-2} a^{-1} (1861–1931) and 290 t km^{-2} a^{-1} (1931–1957) (Rooney and Smith, 1999, their Figure 3) potentially implying that, since WY1983, the cumulative impact of dams, grazing and urban development on area-specific sediment *yield* from the Middle Lagunitas Creek area has been equivalent to yields related to land surface disturbances associated with early Euro-American arrival in the wider catchment. Averaged across the entire catchment area (213 km^2), the 1983–2008 estimate equates to a yield of ~90 t km^{-2} a^{-1}, thus describing a multi-decadal unit yield reduction that can be attributed to regulated flows and reductions in the sediment contributing area.

Locally, the estimated average sub-catchment rates ~200 t km^{-2} a^{-1} ± ~100 t km^{-2} a^{-1} (maximum 405 t km^{-2} a^{-1}) compare well to ‘headwater’ rate estimates obtained from

neighbouring catchments. Lehre (1982) obtained an average unit yield (1971-1974) of 214 t km^{-2} a^{-1} from monitoring in the neighbouring Long Tree Creek catchment (1.74 km^2), reaching a maximum of 691 t km^{-2} a^{-1} in 1973 when a large storm event occurred, and O'Farrell *et al.* (2007) obtained estimates of hillslope erosion for nearby Haypress Creek catchment (0.33km^2) of 224 to 334 t km^{-2} a^{-1} using fallout radionuclides and pond sediment volumes. Contemporary yields for neighbouring Redwood Creek (22.7 km^2), a catchment with relatively limited human influences and extensive conservation management, were estimated at 198 t km^{-2} a^{-1}, reduced from peak historical yields conservatively estimated at 324 t km^{-2} a^{-1}, (Stillwater Sciences, 2004; Gregory and Downs, 2008). In regional comparison, yields from the tectonically active and highly ENSO-influenced ephemeral channels of the Santa Ynez mountains in southern California average 1,500 to 2,700 t km^{-2} a^{-1} (and far higher immediately following significant wildfire, Warrick *et al.*, 2015), and yields exceeding 1,000 t km^{-2} a^{-1} are also estimated for the wet, steepland catchments further north in California (*e.g.*, Kelsey, 1980; Best *et al*., 1995). The estimated yields for Lagunitas Creek and its sub-catchments appear logical in comparison to these other yields.

In terms of trajectory, sediment yield dynamics in the Lagunitas catchment appear to reflect a centennial-scale disturbance cycle related to changes in runoff and sediment supply that has been frequently observed both across the US (*e.g.*, Wolman, 1967; Trimble, 1983, 1999; Pasternak *et al*., 2001, Reusser *et al.*, 2015) and other areas subject to rapid clearance of native vegetation during settlement of non-indigenous populations (*e.g.*, Australia: Fryirs and Brierley, 1999). In Europe such cycles may have had a millennial timeframe and reflect forest clearances or

changing agricultural practices (*e.g.*, Brown, 2009; Verstraeten *et al*., 2009; Broothaerts *et al.*, 2013; Foulds *et al*., 2013). Here, historical maps confirm that rates of catchment sediment delivery were enhanced greatly by land clearances that followed Euro-American settlement in the region: the mouth of Lagunitas Creek advanced more than 1 km into Tomales Bay from 1860 to 1918 and a further 500–800 m along tidal channels in the period 1918–1954 (Niemi and Hall, 1996). Sediment yields probably began to diminish after row crop reductions in the 1930s; comparable changes were observed in neighbouring Stemple Creek where significant decreases in floodplain sedimentation rates occurred after the conversion from row crops to pasture in the 1950s (Ritchie *et al.*, 2004). By the period 1954–1982, the mouth of Lagunitas Creek stabilised in Tomales Bay (Niemi and Hall, 1996), presumably in response to progressive reductions in effective sediment contributing area resulting from the impoundment of Kent Lake (1954) and then Nicasio Reservoir (1961). The recent sediment budget for Lagunitas Creek thus appears consistent with historical accounts, is highly contingent on the legacy imparted by catchment history and, in general, depicts a variation on the classic disturbance curve of sediment supply (Wolman, 1967), adjusted for the presence of large dams.

Insights into fluvial system dynamics of dammed rivers

While, at the catchment scale, the results illustrate the role of channel erosion offsetting sediment yield reductions caused by the progressive disconnection of upstream sediment sources, the distributed sediment budget approach implies anthropogenic changes to each component part of the Lagunitas fluvial system. Hillslope sediment *production* appears to be accelerated on de-forested hillslopes

(**Figure 5**) and in locations with a high density of unpaved roads (*e.g.*, San Geronimo Creek, **Figure 9**). In channels, high rates of production associated with frequent bank failures and channel bed erosion (**Figures 6, 9**) are most logically linked to the impacts of clear water erosion and incision below dams (*e.g.*, Kondolf 1997) and increased flow peakedness resulting from urban developments. Sediment *storage* on steep hillslopes is suspected of having been reduced by land cover changes that have resulted in headward extension of tributary channels, but has certainly been reduced where incision of mainstem channels has switched downstream alluvial areas from being sediment sinks to sediment sources (**Figures 6, 9**). Rates of *movement through storage* have probably increased through several, linked, mechanisms. First, the switch from the primacy of hillslope sediment sources towards channel sediment sources implies an increase in the sediment delivery ratio towards unity; second, channel-stored sediments are likely to be mobile on a near-annual basis whereas hillslope sediments will be far less frequently mobile (as they require a threshold precipitation of 190–200 mm in 24 hours for mobilization; see **Table 1)**, and; third, because channel incision now largely eliminates the prospect of sediments returning to long-term storage as overbank sediments.

Finally, sediment *transfer processes* will have been accelerated by channel network extension and by local channelization of tributaries related to urban development, but perhaps most significantly due to channel incision that causes flood flows to be contained in-bank where they can generate substantial shear stresses for sediment transport. The impact of this latter mechanism on transfer processes is enhanced by the highly bimodal flow regime wherein regulated discharges, largely incapable of transporting significant volumes of bed sediment, are punctuated periodically by

ENSO-related dam spills that release substantial (but still in-bank) flood flows that transport sediment very effectively. Consequently, annual yields are estimated to vary by three-orders of magnitude (from ~400 t in WY1990 to ~61,000 t in WY1998, Stillwater Sciences, 2010) resulting, statistically, in extremely high uncertainty in the average sediment yield near the catchment outlet (PRS gauge: 17,000 ± 19,000 t a^{-1}).

Such internal changes to the component processes of the fluvial system identified here underline the generic utility of a distributed sediment budget over a single estimate of sediment yield. It emphasises, for instance, why the *relative location* of human activities is paramount: potentially very different dynamics may have resulted if the catchment population was centred downstream of the dams, rather than upstream (*cf.* Warrick and Rubin, 2007). Unravelling such nuances demands an approach that is both process-based *and* spatially explicit (see also Verstraeten *et al.*, 2009), and will inevitably require a method for area-based extrapolation (Reid and Dunne, 1996, achieved here using GLUs). However, it also requires a significant appreciation of the historical contingency within the selected catchment (see **Figure 2**) to account for the cumulative changes in intra-catchment sediment functions caused by multiple overlapping and historical human activities.

The specific utility of this distributed sediment budget is in assessing the impact of a highly regulated flow regime (70% regulated at the downstream-most gauge) and moderate urban expansion on fluvial system dynamics. Both of these conditions would be expected to promote channel erosion and incision (Nelson and Booth, 2002; Gregory, 2006). However, because it is generally reasonable to expect

prograding incision downstream of large dams (Petts, 1979; Williams and Wolman, 1984) at a rate relative to the frequency of receiving morphologically effective flow releases (Petts, 1982), the shift in sediment production away from hillslopes and towards mainstem alluvial sediment sources should partially compensate for sediment production losses caused by disconnection of large parts of the catchment (**Figure 8**), at least until alluvial sediment stores are exhausted. Here, compensation has apparently been sufficient for the contemporary sediment yield from the Middle Lagunitas Creek (~300 t km^{-2} a^{-1}) to rival estimated maximum catchment yields caused by deforestation and cropping by early Euro-American settlers.

Such alluvial sediment remobilisation is particularly significant because the combination of near 100% delivery ratio of channel network-derived sediments and reductions in overbank sedimentation potential causes the ratio of catchment sediment production to yield at the catchment mouth to be far closer to unity than it was historically. The consequence is that the catchment efflux may be greater here than in catchments where overall sediment production is higher but colluvial storage and floodplain aggradation act to reduce sediment yields. Compare, for instance, the 84% of catchment sediments exported from Middle Lagunitas Creek (**Figure 8**) to Trimble's (1999) reported residual sediment efflux of 9–32% across three periods for the unregulated agricultural lowland catchment of Coon Creek (360 km^2), or Royall and Kennedy's (2016) yield of 28% from the smaller, steeper, but little disturbed Rocky Cove catchment (2 km^2) in the Blue Ridge Mountains of North Carolina. Eventually, network-wide depletion in alluvial storage is likely to be arrested by bedrock exposure; outcrops in Lagunitas and San Geronimo Creeks may be evidence of this change occurring.

More broadly, if the transformation in fluvial system dynamics indicated by this example applies more generally to regulated rivers, the prevalence of dammed rivers following the global dam building boom of the 1960s (Beaumont, 1978; Graf, 2001) may have caused a world-wide shift in the relative importance of catchment sediment sources away from hillslope sediments with low channel delivery ratios towards high-yielding channel alluvium. Incised rivers with floodplains as sediment sources rather than sediment sinks may thus be the archetypal response to the 'overwhelming' influence of humans in the 'Great Acceleration' of the later Anthropocene. This is not least because parallel arguments could be made for significance of floodplain sediments in rivers responding to channelization (*e.g.*, Darby and Simon, 1999), urban development (Gregory, 2006) or agricultural drainage (Schottler *et al.*, 2014), or those remobilizing 'legacy' sediments deposited following earlier forest clearances and mill damming (e.g., Donovan *et al*., 2015). Channel-derived sediments are estimated here to comprise 57% of the current sediment yield, and 64-90% in channelized rivers of the south-eastern USA (Simon and Rinaldi, 2006, Table 1). As such, calculations of catchment or regional sediment flux over decadal-to-centennial time-scales that do not estimate channel erosion could significantly underestimate total sediment export (at least until alluvial stores are depleted), emphasising that fluvial geomorphological study must always consider morphological changes alongside sediment flux.

Value and implications of uncertainty estimation

Common to analyses of many 'unconstrained' environmental systems, sediment budgets are subject to uncertainties that include unknown attributes of the processes under study, 'noise' that results from human and instrumental measurement errors,

and natural environmental variability. Further, the variety of data sources required to assemble a distributed sediment budget has seen them described as poor candidates for formal uncertainty analysis. Reid and Dunne (2016: 371), for example, comment that "…sediment budgets represent a complex mix of calculations, mapping, measurements, and qualitative inferences, so standard methods of error analysis are rarely applicable". Conversely, uncertainty assessments are recognised as a critical step in best practice evaluation for environmental models in general (Jakeman *et al*., 2006), and vital to ensure 'defensible data reporting and interpretations' in sediment process research in particular (Horowitz, 2017). Nascent approaches to uncertainty assessments in distributed sediment budgets vary according to whether the budget is based on direct monitoring (Evans and Warburton, 2005), modelling (Wilkinson *et al*., 2009), catchment-historical data (Royall and Kennedy, 2016) or channel-only assessments (e.g., Grams and Schmidt, 2005; Shao *et al*., 2015). Here, attempts to control for *accuracy* focused on representing relevant catchment processes, corroborating estimated point yields against several independent measures, and bounding the budget in an explicit temporal and spatial framework. Assessment of *precision* in the budget was achieved by quantifying potential errors related to direct measurement, field interpretation and model sensitivity, cognisant that this procedure intrinsically incorporates natural environmental variability in addition to error sources.

As sediment budget mass balances are highly simplified representations of complex natural systems (Hinderer, 2012), and because error propagation associated with the numerous data inputs makes high precision over large spatial extents inherently unlikely, uncertainties are likely to be intrinsically high. However, as uncertainty

assessments are so rarely undertaken for sediment budgets, there is no consensus about acceptable or typical error magnitudes, reinforcing the importance of focusing on matters of accuracy in terms of process representation and extrapolation. Further, the large error estimates associated with both corroborating methods emphasize that sediment yields in geomorphology are always subject to high variability when measured over significant spatial extents, whether part of a sediment budget or not. Here, point yield estimates from extrapolated GLUs for the middle Lagunitas catchment are, with one exception, within ± 65% of gauging station data and bathymetric estimation, and compare well with values reported from neighbouring catchments. However, spatially, the apparently systematic errors in the yield estimates derived from different methods (**Table 6**) reflect that the GLU extrapolation process still greatly simplifies the complexity of hillslope-channel sediment transfer processes, despite being based on a lithology-slope-land cover discretisation that is frequently recommended for stratifying geomorphological processes (*e.g.*, Reid and Dunne, 1996; Montgomery, 1999; de Vente *et al.*, 2007; Warrick and Mertes, 2009). Further, temporal budget precision is (and will always remain) constrained by the sampling frequency associated with aerial photographs, cross-section surveys, and other periodic surveys utilised in catchment historical budgets. This study highlights the inherent limitations of accuracy and precision that are rarely reported for sediment budgets.

One significant benefit associated with a structured uncertainty assessment is the identification of specific high-magnitude error sources that could be targeted in future research aimed at improving sediment budget precision. Here, for instance, the average ±73% error estimated for discrete sources of hillslope sediment production

results largely from the standard error associated with the area-to-volume relationship of field-sampled slides and gullies (± 80%) used for determining erosion volume from sources detected using aerial photography. Repeat high resolution scanning of slides and gullies might improve such extrapolation. For channel bed erosion estimates (± 54%) the single greatest individual source of error was attributed to field based estimates of incision (± 50%). As such, regular monitoring of channel bed topography via cross-sections, low-flow bathymetric surveys or other approaches (see Soar *et al*., 2017), every few years, could be the single most effective means of improving volumetric precision for this sediment budget and others highly dependent on channel sediment sources. More generically, a considerable challenge still remains for geomorphology in better understanding the temporal persistence of significant impact by legacy factors, an attribute that is likely to be highly variable per catchment.

According to Refsgaard *et al*. (2007), and implied here in the context of sediment budgets, *epistemic* uncertainties associated with framing and parameterising the budget, specifying inputs and data collection methods and understanding the relevant system dynamics, are all reducible by undertaking more studies, whereas *stochastic* uncertainty associated with inherent natural variability is non-reducible. Reducing the epistemic uncertainty associated with distributed, process-based sediment budgets constructed for decadal time scales, therefore, requires a greatly expanded collection of geomorphic process data to improve the accuracy of process estimates, better extrapolation methods to improve up-scaling associated with sparse data, and the adoption of new measurement technologies to improve the precision, resolution and frequency of data points. Even so, the ultimate precision of

process estimates in sediment budgets will remain constrained by instrument precision and data resolution associated with the earliest data sources. Accuracy concerns are best addressed using an inclusive and explicit organisational framework for process rate estimation that will highlight any data 'surprises'. Here, for instance, the significance of channel-based erosion sources would have been overlooked had the budgeting relied solely on a terrain-based approach. Generic guidelines for best practice stemming from this research include (1) ensuring accuracy by representing relevant processes, (2) setting an explicit temporal context for which to interpret historical legacy and climate effects, (3) incorporating a method for spatial extrapolation to ensure catchment coverage, (4) utilising available methods for independent corroboration and, (5) constraining precision through characterising measurement error and intrinsic natural variability.

6. CONCLUSION

Sediment budgets have great potential in fluvial geomorphology and natural resource management (Slaymaker 2003, 2008; Reid and Dunne, 2016) but are rarely evaluated for their interpretative power or subjected to formal uncertainty analyses. Here, a distributed, process-based budget for the effective sediment contributing portion of the highly regulated Lagunitas Creek (64.4 km^2) in coastal California has provided a structured and enumerated interpretation of the cumulative and multi-faceted impacts of human activities on fluvial sediment dynamics. Decadal-scale sediment yield from the effective contributing area of ~300 t km^{-2} a^{-1} are similar to reported maximum rates of delivery associated with land disturbances during early Euro-American settlement of the region. Each component part of the

fluvial sediment system has been altered by human action – of particular note, sediment delivery is now focused predominantly on channel incision and bank failure processes (57% of the delivered sediment) rather than hillslope erosion (34%, **Figure 9**), which explains a high delivery ratio to the catchment mouth (~85% of ~24,000 t a^{-1}). Given the world-wide prevalence of incised rivers as a response to flow regulation, channelization and urbanization, contemporary sediment budgets that do not account for changes in alluvial storage may significantly misrepresent sediment yields.

While distributed, process-based sediment budgets are not readily amenable to formal error analyses (Evans and Warburton, 2005, Hinderer, 2012; Reid and Dunne, 1996, 2016), an approach was developed here to assess both accuracy and precision through a combination of independent corroboration and error propagation. Results suggest that the sediment budget components were precise to around ± 50% (**Table 4**) and the resulting yields to around ± 30% (**Table 5**). Corroboration with independent data suggested that the area-extrapolated results were within ± 30% over larger spatial extents (**Table 6**), which was perhaps surprising given the extreme variability in annual flow conditions typical to this catchment (standard deviation on the average annual gauged yields of >100%, **Table 6**). Sub-catchment yields compared favourably to those in neighbouring catchments (Lehre, 1982; O'Farrell, 2007) and to historical data for the Lagunitas catchment collected by other means (Niemi and Hall, 1996; Rooney and Smith, 1999). Structured uncertainty assessments also highlight where targeted research might most profitably improve budget precision. For incised rivers, more frequent and higher resolution channel surveys are critical.

Evidence here suggests that a historically-contingent, process-based and distributed sediment budget can provide valuable understanding of intra-catchment fluvial system dynamics under conditions of complex human influence. In this regard, the spatially intricate, incision-led and high-unit yielding fluvial sediment dynamics of Lagunitas Creek may be typical of catchments subject to dam building, channelization and urbanization since the onset of the 'Great Acceleration' phase of the proposed Anthropocene epoch (*i.e.*, since about 1950). Such changes contrast with accelerated rates of alluviation that typically result from initial land clearances associated with rapid settlement (*e.g.*, as classically illustrated by Trimble, 1999). Catchment-historical sediment budgets require the use of secondary data for which there can be little quality control, but using uncertainty assessments can help demonstrate defensible data collection protocols (Horowitz, 2017) that underscore the applicability and societal relevance of fluvial geomorphology. Transparent uncertainty assessments are particularly important when environmental models are used in decision support (Uusitalo *et al*., 2015). For sediment budgets, this might include determining causes of sediment impairment under the US Clean Water Act, or setting historically-relevant baselines of 'hydromorphological' alteration as the basis for remedial actions under the European Water Framework Directive. Although challenging to construct, uncertainty-bound sediment budgets have significant value in avoiding the simplistic enumeration of cumulative impacts on fluvial systems dynamics associated with multiple, spatially- and temporally-overlapping human activities typical of the proposed Anthropocene period.

7. ACKNOWLEDGMENTS

This research was facilitated by grants to the Marin County Department of Public Works, San Francisco Estuary Project and the Association of Bay Area Governments. We are indebted to Bill Dietrich for critical reviews of reports produced as part of this study, and to Derek Booth, Neil Roberts, Sara Rathburn and three anonymous referees for critical reviews of this manuscript. We are very grateful to Marin Municipal Water District, Marin County Open Space District, California Department of Parks and Recreation, and the National Park Service for providing land access, logistical support, and historical data sources. Harry Appelton, Laurel Collins, Jenny Curtis, Leslie Ferguson, Barry Hecht, Jill Marshall, Liza Prunske, and Matt Smeltzer provided useful data, advice and research support. Data collection and analysis was assisted by Sayaka Araki, Sebastian Araya, Dino Bellugi, Ronna Bowers, Jim Chayka, Yantao Cui, Liz Gilliam, Gina Lee, Evan Lue, Eric Panzer, Rafael Real de Asua, Jay Stallman and John Wooster. Cartographic assistance was provided by Plymouth University Geomapping Unit.

8. REFERENCES

Beaumont P. 1978. Man's impact of river systems: a worldwide review. *Area* **10**: 38-41.

Best D, Kelsey H, Hagans D, Alpert M. 1995. Role of fluvial hillslope erosion and road construction in the sediment budget of Garrett Creek, Humboldt County, California. In *Geomorphic processes and aquatic habitat in the Redwood Creek basin, northwestern California*, Nolan K, Kelsey H, Marron D. (eds) US Geological Survey Professional Paper 1454: Washington DC: M1-M9.

Beighley RE, Dunne T, Melack JM. 2005. Understanding and modeling basin hydrology: interpreting the hydrogeological signature. *Hydrological Processes* **19**: 1333-1353.

Blake MC, Graymer RW, Jones DL. 2000. Geologic map and map database of parts of Marin, San Francisco, Alameda, Contra Costa, and Sonoma counties, California. US Geological Survey Miscellaneous Field Studies MF-2337: Washington DC.

Booth DB, Leverich GT, Downs PW Dusterhoff SR, Araya S. 2014 A method for a spatially explicit representation of sub-watershed sediment yield, southern California, USA, *Environmental Management*, **53**: 968–984.

Broothaerts N, Verstraeten G, Notebaert B, Assendelft R, Kasse C, Bohncke S and Vandenberghe J. 2013 Sensitivity of floodplain geoecology to human impact: A Holocene perspective for the headwaters of the Dijle catchment, central Belgium, *The Holocene* **23**: 1403–1414.

Brown AG. 2009. Colluvial and alluvial response to land use change in Midland England: An integrated geoarchaeological approach. *Geomorphology* **108**: 92–106.

Brown AG, Tooth S, Bullard JE, Thomas DSG, Chiverrell RC, Plater AJ, Murton J, Thorndycraft V, Tarolli P, Rose J, Wainwright J., Downs PW, Aalto R. 2017. The Geomorphology of the Anthropocene: emergence, status and implications, *Earth Surface Processes and Landforms*, **42**:71–90.

Brown AG, Tooth S, Chiverrell RC, Rose J, Thomas DSG, Wainwright J, Bullard JE, Thorndycraft V, Aalto R, and Downs PW. 2013. The Anthropocene: is there a geomorphological case? *Earth Surface Processes and Landforms* **38**: 413-434.

CGS (California Geological Survey). 2002. California geomorphic provinces. Note 36, California Geological Survey: Sacramento.

Cleveland WS. 1979. Robust locally weighted regression and smoothing scatterplots. *Journal of the American Statistical Association* **74**: 829–837.

Croke J, Mockler S, Hairsine P, Fogarty P. 2006. Relative contributions of runoff and sediment from sources within a road prism and implications for total sediment delivery, *Earth Surface Processes and Landforms* **31**: 457-468.

Crutzen PJ and Steffen W. 2003 How long have we been in the Anthropocene era? *Climatic Change* **61**: 251–257.

Curtis JA. 2007. Summary of optical-backscatter and suspended-sediment data, Tomales Bay Watershed, California. Water years 2004, 2005, and 2006. US Geological Survey Scientific Investigations Report 2007-5224: Washington DC.

Darby SE, Simon A. 1999. (eds). *Incised River Channels: Processes, Forms, Engineering and Management*. J. Wiley and Sons Ltd, Chichester.

de Moor J, Verstraeten G. 2008. Alluvial and colluvial sediment storage in the Geul River catchment (The Netherlands) — combining field and modelling data to construct a Late Holocene sediment budget. *Geomorphology* **95**: 487–503.

de Vente J, Poesen J, Arabkhedri M, Verstraeten G. 2007. The sediment delivery problem revisited, *Progress in Physical Geography* **31**: 155–178.

Dietrich WE, Dunne T, Humphrey NF, Reid LM. 1982. Construction of sediment budgets for drainage basins. In *Workshop on sediment budgets and routing in forested drainage basins*, Swanson FJ, Janda RJ, Dunne T, Swanston DN. (eds), US Forest Service Pacific Northwest Forest and Range Experiment Station General Technical Report PNW-141: Portland: 5–23.

Dietrich WE, Reiss R, Hsu M-L, Montgomery DR. 1995. A process-based model for colluvial soil depth and shallow landsliding using digital elevation data.

Hydrological Processes **9**: 383–400.

Dietrich WE, Bellugi DG, Sklar LS, Stock JD, Heimsath AM, Roering JJ. 2003. Geomorphic transport laws for predicting landscape form and dynamics. In *Prediction in Geomorphology*, Wilcock PR, Iverson RM, (eds). Geophysical Monograph 135, American Geophysical Union: Washington DC.

Donovan M, Miller A, Baker M, Gellis A. 2015. Sediment contributions from floodplains and legacy sediments to Piedmont streams of Baltimore County, Maryland, *Geomorphology* **235**: 88-105.

Downs PW, Gregory KJ, 2004. *River Channel Management: Towards Sustainable Catchment Hydrosystems*. Arnold: London.

Downs PW, Dusterhoff SR, Sears WA. 2013. Reach-scale channel sensitivity to multiple human activities and natural events: Lower Santa Clara River, California, USA, *Geomorphology* **189**: 121-134.

Evans M, Warburton J. 2005. Sediment budget for an eroding peat-moorland catchment in northern England, *Earth Surface Processes and Landforms* **30**: 557–577.

Fischer DT, Smith SV, Churchill RR. 1996. Simulation of a century of runoff across the Tomales Bay Watershed, Marin County, California. *Journal of Hydrology* **186**: 253–273.

Foulds SA, Macklin MG, Brewer PA. 2013. Agro-industrial alluvium in the Swale catchment, northern England, as an event marker for the Anthropocene, *The Holocene* **23**: 587-602.

Fryirs K, Brierley GJ. 1999. Slope-channel decoupling in Wolumba catchment, N.S.W., Australia: the changing nature of sediment sources following European settlement. *Catena* **35**: 41-63.

Graf WL, 2001. Damage control: restoring the physical integrity of America's rivers. *Annals of the Association of American Geographers* **91**: 1-27.

Grams PE, Schmidt JC. 2005 Equilibrium or indeterminate? Where sediment budgets fail: sediment mass balance and adjustment of channel form, Green River downstream from Flaming Gorge Dam, Utah and Colorado, *Geomorphology* **71**: 156–181.

Gregory KJ. 2006. The human role in changing river channels, *Geomorphology* **79**: 172–191.

Gregory KJ, Downs PW. 2008. The sustainability of restored rivers: catchment-scale perspectives on long-term response, in *River Restoration: managing the uncertainty in restoring physical habitat,* Darby SE, Sear DA. (eds.), Chichester: J. Wiley & Sons: 253-286.

Heimsath AM. 1999. The soil production function. Unpublished PhD Dissertation. University of California, Berkeley.

Hicks DM, Gomez B, Trustrum NA. 2000. Erosion thresholds and suspended sediment yields, Waipaoa River Basin, New Zealand, *Water Resources Research*, **36**: 1129-1142.

Hinderer M. 2012. From gullies to mountain belts: A review of sediment budgets at various scales, *Sedimentary Geology*, doi:10.1016/j.sedgeo.2012.03.009.

Hooke RLeB. 2000. On the history of humans as geomorphic agents. *Geology* **28**: 843-846.

Horowitz AJ. 2017. A question of uncertainty. *Hydrological Processes* **31**:2314–2315.

Jakeman AJ, Letcher RA, Norton JP. 2006. Ten iterative steps in development and evaluation of environmental models, *Environmental Modelling and Software*, **21**: 602-614.

James LA, Rathburn SL, Whittecar GR. 2009. Introduction: managing rivers with broad historical changes and human impacts. In *Management and Restoration of Fluvial Systems with Historical Changes and Human Impacts*, James LA, Rathburn SL, Whittecar GR. (eds.) Geological Society of America Special Paper 451: Boulder CO: v-x.

James LA. 2010. Secular sediment waves, channel bed waves, and legacy sediment, *Geography Compass*, **4**: 576–598.

Jennings CW. 1994. Fault activity map of California and adjacent areas (with location and ages of recent volcanic eruptions). California Geological Data Map Series, Map No. 6. Scale 1:750,000. California Division of Mines and Geology: San Francisco.

Juracek KE. 2006. A comparison of approaches for estimating bottom-sediment mass in large reservoirs, US Geological Survey Scientific Investigations Report 2006–5168: Washington DC.

Keefer DK. 1984. Landslides caused by earthquakes. *Geological Society of America, Bulletin* **95**: 406-421.

Kelsey HM. 1980. A sediment budget and an analysis of geomorphic process in the Van Duzen River basin, north coastal California. *Geological Society of America, Bulletin* **91**: 190–195.

Kondolf GM. 1997. Hungry water: effects of dams and gravel mining on river channels. *Environmental Management* **21**: 533–551.

Kondolf GM, Matthews WVG. 1991. Unmeasured residuals and sediment budgets: a cautionary note, *Water Resources Research* **27**: 2483-2486.

Lehre AK. 1982. Sediment budget of a small Coast Range drainage basin in north-central California. In *Workshop on sediment budgets and routing in forested drainage basins*, Swanson FJ, Janda RJ, Dunne T, Swanston DN. (eds), US Forest Service Pacific Northwest Forest and Range Experiment Station General Technical Report PNW-141: Portland: 67–77.

Lewin J. 2013. Enlightenment and the GM floodplain, *Earth Surface Processes and Landforms* **38**: 17–29.

Loader C. 1999. *Local Regression and Likelihood*, Springer-Verlag: New York.

MacDonald LH, Sampson RW, Anderson DM. 2001. Runoff and road erosion at the plot and road segment scales, St John, US Virgin Islands, *Earth Surface Processes and Landforms* **26**: 251-272.

Macklin MG, Lewin J. 2008. Alluvial responses to the changing Earth system. *Earth Surface Processes and Landforms* **33**: 1374-1395.

Meybeck M. 2003. Global analysis of river systems: from Earth system controls to Anthropogene syndromes. *Philosophical Transactions of the Royal Society B: Biological Sciences* **358**: 1935–1955.

Minear JT. Kondolf GM. 2009. Estimating reservoir sedimentation rates at large spatial and temporal scales: A case study of California, *Water Resources Research* **45**: W12502, doi:10.1029/2007WR006703.

Montgomery DR. 1999. Process domains and the river continuum. *Journal of the American Water Resources Association* **35**: 397–410.

Montgomery DR, Buffington JR. 1997. Channel-reach morphology in mountain drainage basins. *Geological Society of America Bulletin*, **109**: 596-611.

Murthy BN. 1977. Life of reservoir. Technical Report No. 19, Central Board of Irrigation and Power (CBIP), New Delhi.

NCASI (National Council for Air and Stream Improvement, Inc.). 2005. Technical documentation for SEDMODL, version 2.0 road erosion/ delivery model. NCASI: Durham NC.

Nelson EJ, Booth DB. 2002. Sediment sources in an urbanizing, mixed land-use watershed, *Journal of Hydrology* **264**: 51-68.

Niemi TM, Hall NT. 1996. Historical changes in the tidal marsh of Tomales Bay and Olema Creek, Marin County, California. *Journal of Coastal Research* **12**: 90–102.

Notebart B, Verstraeten G. 2010. Sensitivity of West and Central European river systems to environmental changes during the Holocene: A review. *Earth-Science Reviews* **103**: 163–182.

NRCS (Natural Resources Conservation Service). 2007. Soil Survey Geographic (SSURGO) database. Available at: http://soildatamart.nrcs.usda.gov/.

O'Farrell C, Heimsath A, Kaste J. 2007. Quantifying hillslope erosion rates and processes for a coastal California landscape over varying timescales. *Earth Surface Processes and Landforms* **32**: 544–560.

Owens J, Shaw D, Hecht B. 2007. Annual hydrologic record and sediment-transport measurements for San Geronimo Creek at Lagunitas Road, Marin County, California, data report for water year 2007. Consulting report prepared for Marin Municipal Water District by Balance Hydrologics, Inc.

Pasternak GB, Brush GS, Hilgartner WB. 2001. Impact of historic land-use change on sediment delivery to a Chesapeake Bay subestuarine delta, *Earth Surface Processes and Landforms* **26**: 409–427.

Petts GE. 1979. Complex response of river channel morphology subsequent to reservoir construction. *Progress in Physical Geography* **3**: 329-362.

Petts GE. 1982. Channel changes within regulated rivers. In *Papers in Earth Studies*, Adlam BH, Fenn CR, Morris L. (eds), Geobooks: Norwich: 117-142.

Refsgaard JC, Van der Sluijs JP, Høberg AL. Vanrolleghem PA. 2007. Uncertainty in

the environmental modelling process – a framework and guidance, *Environmental Modelling & Software* **22**: 1543-1556.

Reid LM, Dunne T. 1996. *Rapid Evaluation of Sediment Budgets*. Catena Verlag: Reiskirchen.

Reid LM, Dunne T. 2016. Sediment budgets as an organizing framework in fluvial geomorphology. In *Tools in Fluvial Geomorphology*, Kondolf GM, Piegay H. (eds), J. Wiley & Sons: Chichester: 357-380.

Reneau SL, Dietrich WE, Wilson CJ, Rogers JD. 1984. Colluvial deposits and associated landslides in the northern S.F. Bay Area, California, USA, Proceedings IV International Symposium on Landslides, Toronto, pp. 425-430.

Reusser L, Bierman P, Rood D. 2015. Quantifying human impacts on rates of erosion and sediment transport at a landscape scale, *Geology*, **43**: 171-174, doi:10.1130/G36272.1

Ritchie JC, Finney VL, Oster KJ, Ritchie CA. 2004. Sediment deposition in the flood plain of Stemple Creek watershed, northern California. *Geomorphology* **61**: 347–360.

Roering JJ, Kirchner JW, Dietrich WE. 1999. Evidence for nonlinear, diffusive sediment transport on hillslopes and implications for landscape morphology, *Water Resources Research*, **35**: 853-870.

Roering JJ, Kirchner JW, Sklar LS, Dietrich WE. 2001. Hillslope evolution by nonlinear creep and landsliding: an experimental study, *Geology* **29**: 143-146.

Rooney JJ, Smith SV. 1999. Watershed landuse and bay sedimentation. *Journal of Coastal Research* **15**: 478–485.

Royall D. Kennedy L 2016. Historical erosion and sedimentation in two small watersheds of the southern Blue Ridge Mountains, North Carolina, USA, *Catena* **143**: 174-186.

Ruddiman WF, Ellis EC, Kaplan JO, Fuller DQ. 2015 Defining the epoch we live in. Is a formally designated “Anthropocene” a good idea? *Science* **348:** 38-39.

Schottler SP, Ulrich J, Belmont P, Moore R, Lauer JW, Engstrom DR. Almendinger JE. 2014. Twentieth century agricultural drainage creates more erosive rivers, *Hydrological Processes* **28**: 1951-1961.

SFBRWQCB (San Francisco Bay Region Water Quality Control Board). 2002. Surface water ambient monitoring program (SWAMP). Final Workplan 2001–2002, SFBRWQCB: Oakland, CA.

Sear DA, Newson MD, Brookes A. 1995. Sediment-related river maintenance: the role of fluvial geomorphology. *Earth Surface Processes and Landforms* **20**: 629–647.

Shao W, Shi, C, Fan X, Zhou, Y, Bai B. 2016 Sediment budgets for a sediment-laden river: the lower Wei River in the period 1960–1990. *Earth Surface Processes and Landforms* **40**: 414-426.

Simon A, Rinaldi M. 2006. Disturbance, stream incision, and channel evolution: The roles of excess transport capacity and boundary materials in controlling channel

response, *Geomorphology*, **79**: 361-383.

Slagel MJ, Griggs GB. 2008. Cumulative losses of sand to the California coast by dam impoundment, *Journal of Coastal Research* **24**: 571–584.

Slaymaker O. 2003. The sediment budget as conceptual framework and management tool, *Hydrobiologica* **494**: 71-82.

Slaymaker O. 2008. The future of geomorphology, *Geography Compass* **3**: 329-349

Soar PJ, Wallerstein NP, Thorne CR. 2017. Quantifying river channel stability at the basin scale, Water, **9**: 133; doi:10.3390/w9020133.

Stetson Engineers, Inc. 2002. San Geronimo Creek Watershed sediment source sites assessment and evaluation for the San Geronimo Creek Watershed Planning Program. Stetson Engineers: San Rafael, CA, for Marin Municipal Water District: Corte Madera, CA.

Stillwater Sciences. 2004. Sediment budget for Redwood Creek watershed, Marin County, California. Stillwater Sciences: Berkeley, CA for California for Golden Gate National Recreation Area, San Francisco, CA.

Stillwater Sciences. 2010. Taking action for clean water – Bay Area Total Maximum Daily load Implementation: Lagunitas Creek sediment budget. Stillwater Sciences: Berkeley CA, for San Francisco Estuary Project / Association of Bay Area Governments: Oakland, CA.

Snyder NP, Rubin DM, Alpers CN, Childs JR, Curtis JA, Flint LE, Wright SA. 2004. Estimating accumulation rates and physical properties of sediment behind a dam: Englebright Lake, Yuba River, northern California. *Water Resources Research* **40**: W11301, doi:10.1029/2004WR003279.

Strahler AN. 1952. Dynamic basis of geomorphology. *Geological Society of America, Bulletin* **63**: 923–938.

Taylor JR, 1997, An Introduction to Error Analysis (2d ed.), University Science Books: Sausalito.

TBWC (Tomales Bay Watershed Council). 2003. The Tomales Bay watershed stewardship plan: a framework for action, TBWC: Pt. Reyes Station: CA.

Trimble SW. 1983. A sediment budget for Coon Creek basin in the Driftless Area, Wisconsin, 1853–1977. *American Journal of Science* **283:** 454–474.

Trimble SW. 1999. Decreased rates of alluvial sediment storage in the Coon Basin, Wisconsin, 1975–93. *Science* **285**: 1244–46.

Trimble SW. 2009. Fluvial processes, morphology and sediment budgets in the Coon Creek Basin, WI, USA, 1975–1993, *Geomorphology* **108**: 8-23.

Uusilato L, Lehikoinen A, Helle I, Myrberg K. 2015. An overview of methods to evaluate uncertainty of deterministic models in decision support, *Environmental Modelling & Software* **63**: 24–31

Vanmaerke M, Kettner AJ, Van Den Eeckhaut M, Poesen J, Mamaliga A, Verstraeten G, Rãdoane M, Obreja F, Upton P, Syvitski JPM, Govers G. 2014. Moderate seismic activity affects contemporary sediment yields, *Progress in Physical Geography* **38**: 145–172.

Verstraeten G, Rommens T, Peeters I, Poesen J, Govers G, Lang A. 2009. A temporarily changing Holocene sediment budget for a loess-covered catchment (central Belgium). *Geomorphology* **108**: 24–34.

Warburton J. 2011. Sediment transport and deposition. In *The SAGE Handbook of Geomorphology*, Gregory KJ, Goudie AS. (eds). SAGE Publications: London: 326-342.

Warrick JA. Melack JM, Goodridge BM. 2015. Sediment yields from small, steep coastal watersheds of California, *Journal of Hydrology: Regional Studies* **4**: 516-534.

Warrick JA. Mertes LAK. 2009. Sediment yield from the tectonically active semiarid Western Transverse Ranges of California, *Geological Society of America, Bulletin* **121**: 1054-1070.

Warrick JA, Mertes LAK, Washburn L, Siegel DA. 2004, A conceptual model for river water and sediment dispersal in the Santa Barbara Channel, California, *Continental Shelf Research* **24**: 2029–2043.

Warrick JA, Rubin DM. 2007. Suspended-sediment rating curve response to urbanization and wildfire, Santa Ana River, California, *Journal of Geophysical Research – Earth Surface* 112: F02018, doi:10.1029/2006JF000662.

Wasson RJ. 2002. Sediment budgets, dynamics, and variability: new approaches and techniques. In Dyer FJ, Thorns MC, Olley JM. (eds). *The Structure, Function and Management Implications of Fluvial Sedimentary Systems.* Proceedings of an international symposium held at Alice Springs, Australia. September 2002. IAHS Publication 276: 471–478.

Wemple BC, Swanson FJ, Jones JA. 2001. Forest roads and geomorphic process interactions, Cascade Range, Oregon, *Earth Surface Processes and Landforms* **26**: 191-204.

Wentworth CM. 1997. General distribution of geologic materials in the San Francisco Bay region, California: a digital map database based. US Geological Survey Open-File Report OFR 97-74: Washington DC.

Williams GP, Wolman MG. 1984. Downstream effects of dams on alluvial rivers. US Geological Survey Professional Paper 1286: Washington DC.

Wilkinson BH. 2005. Humans as geologic agents: a deep-time perspective. *Geology* **33**: 161–164.

Wilkinson SN, Prosser IP, Rustomji P. Read AM. 2009. Modelling and testing spatially distributed sediment budgets to relate erosion processes to sediment yields. *Environmental Modelling & Software* **24**:489–501.

Wilson RC, Jayko A. 1997. Preliminary maps showing rainfall thresholds for debris-flow activity, San Francisco Bay region, California. US Geological Survey Open-File Report 97-745F: Washington DC.

Wolock DM, Winter TC, McMahon G. 2004. Delineation and evaluation of hydrologic-landscape regions in the United States using geographic information system tools and multivariate statistical analyses. *Environmental Management* **34** (Suppl. 1): S71–S88, doi 10.1007/s00267-003-5077-9.

Wolman MG. 1967. A Cycle of Sedimentation and Erosion in Urban River Channels. *Geografiska Annaler* **49A**: 385-395.

Yoo, K, Amunson R, Heimsath AM, Dietrich WE. 2005. Erosion of upland hillslope soil organic carbon: coupling field measurement with a sediment transport model. *Global Biogeochemical Cycles* **19**, GB3003, doi: 10/1029/2004GF002271

Youd, T. L. and S. N. Hoose. 1978. Historic ground failures in northern California triggered by earthquakes. US Geological Survey Professional Paper 993: Washington DC.

Zalasiewicz J, Williams M, Steffen W, Crutzen P. 2010. The new world of the Anthropocene. *Environmental Science and Technology* **44**: 2228-2231.